ANALYSIS OF EROSION IN HYDRO TURBINES

A DISSERTATION

Submitted in partial fulfillment of the
requirements for the award of the degree
of
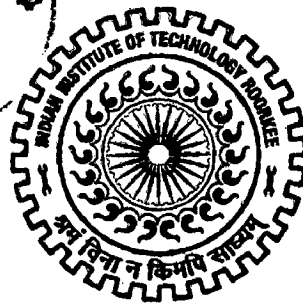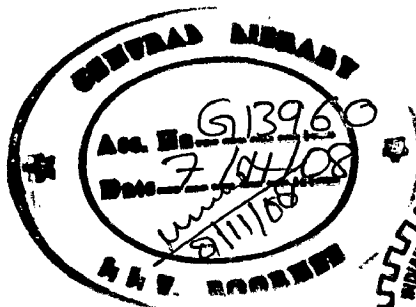MASTER OF TECHNOLOGY
in
ALTERNATE HYDRO ENERGY SYSTEMS

By
RATNENDRA SINGH

ALTERNATE HYDRO ENERGY CENTRE
INDIAN INSTITUTE OF TECHNOLOGY ROORKEE
ROORKEE - 247 667 (INDIA)
JUNE, 2008

CANDIDATE'S DECLARATION

I hereby certify that the report which is presented in this dissertation work, "**ANALYSIS OF EROSION IN HYDRO TURBINES** ", in partial fulfillment of the requirement for the award of the degree of **MASTER OF TECHONOLOGY IN ALTERNATE HYDRO ENERGY SYSTEMS**, submitted in Alternate Hydro Energy Center, Indian Institute of Technology, Roorkee is an authentic record of my own work carried out during the period from July, 2006 to June, 2008 under the supervision of **Shri S. K. SINGHAL** , Senior Scientific Officer, Alternate Hydro Energy Center, Indian Institute of Technology, Roorkee and **Dr. R. P . Saini** , Associate Professor Alternate Hydro Energy Center, Indian Institute of Technology, Roorkee.

I have not submitted the matter embodied in the Project for award of any other degree.
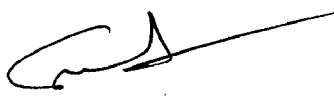
Date:27 June, 2008

Place: Roorkee

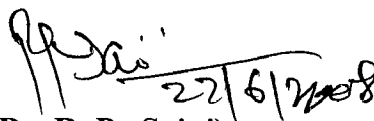(RATNENDRA SINGH)

CERTIFICATE

This is to certify that the above statement made by the candidate is correct to the best of my knowledge

(Shri . S .K Singal)
Senior Scientific Officer
Alternate Hydro Energy Centre
Indian Institute of Technology
Roorkee – 247667

(Dr. R. P . Saini)
Associate Professor,
Alternate Hydro Energy Centre
Indian Institute of Technology
Roorkee - 247667

ACKNOWLEDGEMENTS

It is with great pleasure that I take this opportunity to bow my head in respect and gratitude for all those who helped me in making this dissertation a success . I am in dearth of words to express myself in such a joyous moment .

I heartily like to acknowledge my sincere gratitude and indebtedness to **Shri S. K. Singal** Sr. Scientific Officer, Alternate Hydro Energy Centre, I.I.T. Roorkee And **Dr R P Saini** ,Associate Professor, Alternate Hydro Energy Centre, I.I.T. Roorkee for the precious guidance and kind information, continuous help and the affectionate treatment. No rhapsody or rhetoric eloquence can replace of what they had done for me and the way they have helped me in bringing out this dissertation . I will always be indebted to them all our long life.

I wish to express my profound gratitude to **Shri Arun Kumar**, Head, Alternate Hydro Energy Centre, Indian Institute of Technology, Roorkee for providing all the facilities, which have made it possible for me to complete this report. The cooperation they gave is greatly appreciated.

Finally, my sincere regards to my family, friends and staff at the department who have directly and indirectly helped me in making this dissertation a success . I would feel the bliss of a beneficiary by the showers of their benevolent blessings .

RATNENDRA SINGH

ii

ABSTRACT

As it is well known that hydro turbine in a hydro power plant constitutes of one of the most important component and if it is not functioning properly or out of order and maintenance is required than the plant suffers a huge loss in its capacity of power generation which is itself a source of revenue for it and thereby suffering correspondingly huge economic losses. Moreover even one percent loss in efficiency of the turbine due to cavitation / silt erosion is responsible for huge economic losses and revenue to a utility .

For many years, solutions to the problem have been sought with only partial success. Despite advances in hydraulic-laboratory instrumentation and use of large-capacity computers to model three-dimensional flow through a runner, cavitation erosion remains a prime concern to owners of hydropower plants.

In this dissertation cavitation erosion has been dealt in detail. Number of research to establish the empirical relationship to study the effect of cavitation have been developed . Relationship between cavitation intensity and specific speed or power plant turbine sigma (σ_p,Thomma's cavitation factor) were combined for cavitation analysis in hydro turbine .Under the present study a different approach has been taken, using an empirical equation developed by J.L.GORDAN that establishes the setting of a hydraulic turbine with respect to tail water and all these equation have been applied to an actual site Chilla in Rishikesh . Based on IEC cavitation guarantee range different submergence levels , mass loss , efficiency loss and loss in power generation is estimated for the site . Based on the study the loss of power generation due to cavitation erosion and optimum submergence level to minimize cavitation erosion losses have been suggested . The study may also be useful for improving the accuracy of the empirical relations developed earlier .

TABLE OF CONTENTS

CHAPTER	TITLE	PAGE	No.

LIST OF TABLES

LIST OF FIGURES

NOMENCLATURE

SYMBOL	DEFINITION	UNITS
A	Factor applied to plant capacity factor	-
B	Value of atmospheric pressure less water-vapor pressure at tailwater level (m of water head)	m
b	Number of runner blades on turbine	-
C_f	Plant capacity factor, equal to annual generation divided by (installed capacity x 8,760), expressed as a decimal, within a range of 0.1-1.0	-
Cg	Cavitation guarantee factor for a runner	-
D	Runner throat diameter	m
E	Tail water elevation (above sea level)	m
g	acceleration due to gravity	9.81 m/s^2
h	Net head on turbine	m
k	Cavitation index for turbine, expressed as weight of metal lost (kg) per 8,000 hours operation divided by runner diameter squared (ranges from 0 up to about 10)	-

k_1	Cavitation index determined as for k, but for suction side of runner blades only	-
k_2	Turbine casing factor	-
k_3	Draft tube factor	-
O	Turbine full-load output at rated net head	kW
R	Turbine runner factor	-
R_1	Revised turbine runner factor	-
Sa	Actual runner submergence (below tailwater), negative when above tailwater	m
S_t	Theoretical runner submergence	m
T	Water temperature	^0C
V	Gross water velocity through throat of runner with no allowance for deduction of runner hub area	m/s
W	Weight of metal lost per 8,000 hours operation from suction side of runner blades	Kg
γ	Factor that measures difference between actual and calculated runner submergence	-
σ_p	Thoma coefficient	-

$NPSE$	net positive suction energy	Nm/Kg
E	specific energy	Nm/Kg
p_I	suction section pressure	Pa
ρ	density	Kg/m3
C_I	suction section mean velocity	m/s
p_a	downstream-free surface pressure	Pa
p_B	bubble pressure	Pa
p_I	suction section pressure	Pa
p_v	vapour pressure	Pa
Hs	machine setting level	m
ZI	suction section height	m
$Zref$	reference section height	m
ω	angular velocity	rad/s
ψ	pressure coefficient	-
φ	flow coefficient	-

CHAPTER-1

INTRODUCTION AND LITERATURE REVIEW

1.1   INTRODUCTION

1.1.1   General

The industrial revolution which the world experienced nearly two hundred years ago was the epochal shift to the ordinary black coal, an energy rich hydrocarbon that supplemented wood as the primary fuel. The coal was then used to give the power to the industrialists which they used to process steel, propel steamships and energize machines. As the time passed by the demand of energy by the industrialized world increased tremendously and also due to increase of the population. Petroleum and natural gases were than exploited as versatile and high quality energy products. Fifty years later atomic energy was extracted from the enriched Uranium which is used as fuel to nuclear reactors.

Nowadays we have been more dependant on these Non-Renewable sources of energy to meet the demand of the growing population and developing world thereby pressurizing the energy sources like coal, oil, natural gas, uranium. The use of non-renewable fuels threatens our health and environment but also the supply of these fuels is physically limited. On the analysis of rate of increase of future growing demands and the trend the world has been moving, it is explicit that the non-renewable sources of energy cannot fulfill the demand of the growing world and if it goes on than these sources of energy will be depleting thereby leading to an energy crisis.

So in this present scenario we have to move to other sources of energy so as to face the energy crisis and one of the solutions to this may be the use of abundant renewable energy resources around. Renewable energy would play a major role in energy industry of the twenty-first century and beyond. These alternative energy resources will not only help in reducing greenhouse emissions but may also cater the need of world in the next century. The renewable energy sources are solar power, wind power hydroelectric power, biomass materials, geothermal energy, tidal energy, wave energy and hydrogen as fuel cells, among which hydropower is the second largest renewable

source. The renewable energies are not yet economically competitive with fossil fuels but if we consider the health, environmental costs and future energy needs of energy, the price of renewable energy becomes competitive . Although no renewable energy system can single handedly replace oil but together they would share total energy demand and thus become a very important part of the energy mix of the future in which hydroelectric power would play a major role, coming second among renewables after biomass with least number of disadvantages.

1.1.2 Small hydro development in India

The first small hydro project of 130 kW commissioned in the Hills of Darjeeling, West Bengal in 1897. The Sivasamudram Project of 4500 kW was the next to come up in Mysore district, Karnataka in 1902, for supply of power to the Kolar gold mines at 25 Hz. The pace of power development including hydro was rather tardy. The planned development of hydro projects in India was taken up in the post independence era. This means that the 1362 MW capacity (including 508 MW hydro) installed in the country before independence was mainly coming from small- and medium-sized projects. Since focus was laid on large-scale power generation through big hydro, thermal, and nuclear routes; the small hydro power (SHP) potential remained untapped. During the last 10–15 years, however, the necessity for development of SHP has been felt globally due to its various benefits particularly concerning environment, and it has assumed importance in the power development programme with time .

1.1.3 Importance of SHP IN present Scenario of Energy Crisis

Small hydro is environmentally benign, operationally flexible, and suitable for peaking support to the local grid as well as for stand-alone applications in isolated remote areas. Even if we ignore the CO_2 and acid rain abatement costs, etc. of conventional thermal route, small hydro is benevolent on the following known hard facts of economics.

• Levelized cost of generation from small hydro would be less than half that of thermal.

• Their real capital investment is less than that of thermal, considering infrastructural costs (small dams/ diversion structure vis-à-vis large mines/transport of coal) and auxiliary factors (small hydro auxiliary consumption of 0.5 per cent vis-à-vis 10 per cent in case of thermal).

2

• On the basis of project life cycle cost in real terms, inflation-free small hydro becomes several times cheaper than thermal option, due to the following weightage factors and cheaper operational costs with reference to maintenance and zero cost input.

Advantage	Weightage Factor
Double the life of small hydro vis-à-vis thermal	2
An escalation of six per cent per annum in case of thermal over hydro having project life of 60 years and more	8.89
The actual generation in long term comes at least 20 per cent higher than the 75 per cent hydrological dependability	1.2

1.1.4 Small hydro vis-à-vis other renewables

Now let us examine superiority of small hydro even amongst renewables

- It is the highest-density renewable energy source against widely spread and thinly distributed solar energy, biomass, wind resource, etc.

- Its cost of generation is cheapest amongst renewables[1]

Table 1.1 Cost of generation of renewables

Sector	Rs/kWh
Small hydro	1.00–1.50
Cogeneration	1.25–1.50
Biomass power	1.75–2.00
Wind energy	2.00–2.75
Solar PV	10.00–12.00

3

- Small hydro efficiencies are highest amongst renewables [1]

Table 1.2 Efiiciency of different renewables

Sector	Efficiency (per cent)
Small hydro	85-90
Cogeneration	60
Biomass power	35
Wind energy	40
Solar PV	15

- Small hydro has longest project life[1]

Table 1.3 Project life of different renewables

Sector	Life(years)
Small hydro	60
Cogeneration	30
Biomass power	30
Wind energy	20
Solar PV	20

- Small hydro resource is more consistent compared to other renewables like wind, solar, biomass with regard to its availability for power generation. Relatively better capacity factors can be expected. Even run-of-the-river schemes can have small pondage to meet the daily peak requirements of power

1.1.5 BASIC COMPONENTS OF SHP
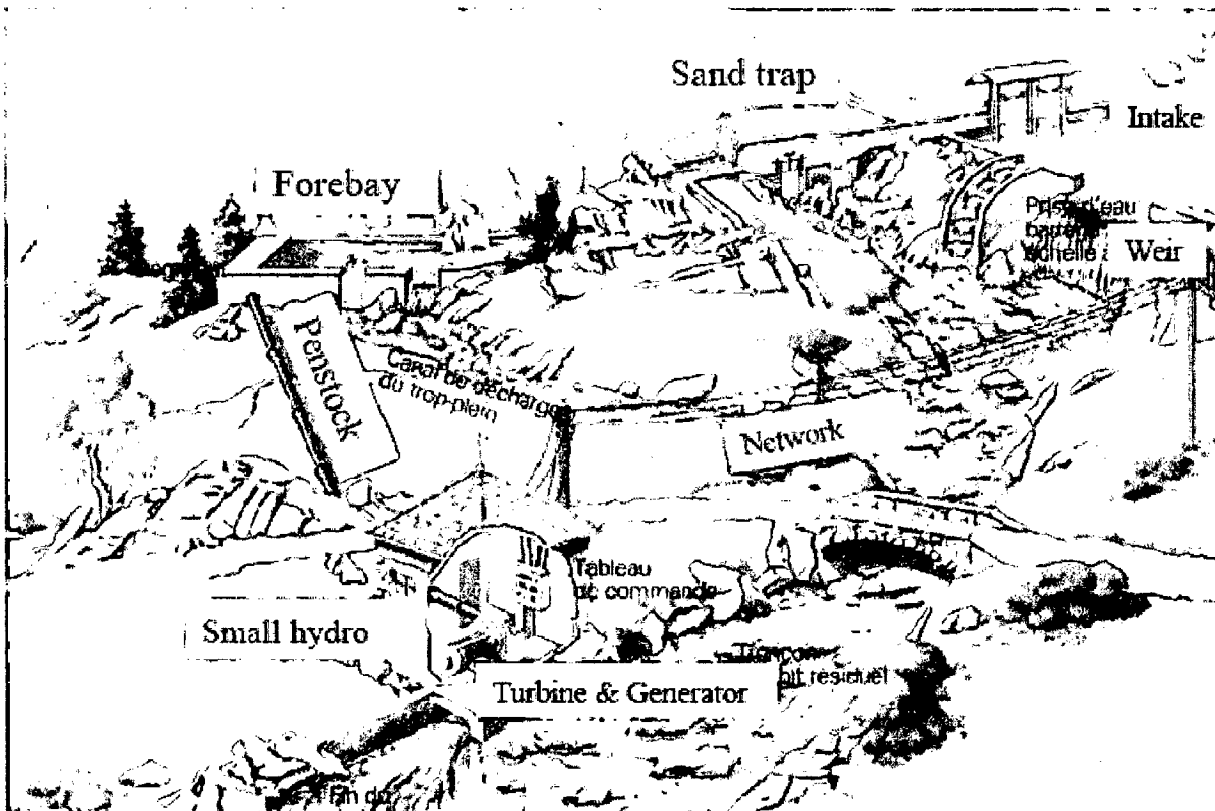
Fig 1.1 Layout of SHP showing its basic components

1.1.6 Importance of turbine in Hydro power plants

A water flow from an upper level to a lower level represents a hydraulic power potential. This power flow can be utilised in a water power plant by conversion to mechanical power on the shafts of turbines. Hydropower machine is the designation used for a machine that directly converts the hydraulic power in a water fall to mechanical power on the machine shaft. This power conversion involves losses that arise partly in the machine itself and partly in the water conduits to and from the machine.

5

The discharge and the net head for turbines differ in wide ranges from one power plant to another. This indicates that not only different types of turbines but also a very large register of sizes of turbines are needed.

The ordinary turbine types in hydro power plants are distinguished in two main groups:

1. Impulse turbines
2. Reaction turbines

This distinction is based on the difference between the two cases of energy conversion in these turbines. Briefly these two ways of energy conversion may be pronounced as follows.

- Basically the flow energy to the *impulse turbines* is completely converted to kinetic energy before transformation in the runner. This means that the flow passes the runner buckets with no pressure difference between inlet and outlet. Therefore only the impulse forces being transferred by the direction changes of the flow velocity vectors when passing the buckets create the energy converted to mechanical energy on the turbine shaft. The flow enters the runner at nearly atmospheric pressure in the form of one or more jets regularly spaced around the rim of the runners. This means that each jet hits momentarily only a fraction or part of the circumference of the runner. For that reason the impulse turbines are also denoted *partial turbines*.[2]

- In the *reaction turbines* two effects cause the energy transfer from the flow to mechanical energy on the turbine shaft. Firstly it follows from a drop in pressure from inlet to outlet of the runner. This is denoted the *reaction part* of the energy conversion. Secondly changes in the directions of the velocity vectors of the flow through the canals between the runner blades transfer impulse forces. This is denoted the *impulse part* of the energy conversion. The pressure drop from inlet to outlet of the runners is obtained because the runners are completely filled with water. Therefore this group of turbines also have been denoted as *full turbines*.[2]

The most commonly used turbines today are:

- Impulse type: *Pelton turbines*
- Reaction type: *Francis turbines*

Kaplan turbines

Bulb turbines

The equation of hydraulic efficiency can now be expressed as

$$\eta = \frac{P_R}{P_n}$$

The power transfer to the runner is further exposed to additional losses before the resulting power P is transferred to the generator shaft. These losses are composed of mechanical friction in the bearings and stuffing boxes, viscous friction from the fluid between the outside of the runner and the covers of the reaction turbines and ventilation or air friction losses of the runner in impulse turbines. Through the space between the covers and the outside of the runner a leakage flow also passes according to the clearances of the labyrinth seals, from the inlet rim to the suction side of the runner. Some energy is also required for operation of the turbine governor, tapping water for sealing boxes, ejectors and cooling of bearings and the governor oil.

On account of all these losses the turbine efficiency is always lower than the hydraulic efficiency. Therefore, at the discharge Q and the power P transferred from the turbine shaft to generator shaft, the turbine efficiency is

$$\eta = \frac{P}{P_n} = \frac{P}{\rho Q g H_n}$$

Usually the maximum efficiency point which is represented by the best operating conditions, is reaching values of say $\eta = 0.93$ to 0.95 of the larger and best reaction turbines. Corresponding values estimated for the hydraulic efficiency $\eta_h = 0.95$ to 0.97. For the best Pelton turbines η_{max} reaches values about 0.92. however this efficiency and performance of turbine is drastically effected by the phenomenon of cavitation and erosion caused due to silt laden water . With both cavitation and sand particles in the flow there is very considerable material removal, much more than would be expected from summing the two individual effects. Cavitation and silt-erosion often co-exist causing severe damage. This effect of cavitation is referred as cavitation enhancement. But the mechanism of this synergetic erosion is still not fully understood yet despite the efforts made in past decades. In this way understanding the cavitation and silt erosion and

their combined effect becomes very important so as to reduce the losses in a Small Hydro Power Plant to a minimum value.

1.1.7 Problem of erosion in hydro turbines

Damages concerning water turbines are caused mainly by cavitation problems, sand erosion, material defects and fatigue. These problems are consequences essentially of high pressures, pressure variations and high water velocities which to some extent depend on the ever prevailing search for a minimizing of the costs of the investments

The erosion in hydro turbines is majorly because of the two factors or it can be said that erosion in hydro turbine is of two types

- Cavitation erosion
- Silt erosion

1.1.7.1 Cavitation

When the pressure in a liquid is lowered down to vapour pressure, cavities are created in the liquid, i.e., bubbles filled with air and vapour. This may occur in the low-pressure regions of the turbines, especially at the outlet of runners and inlet of the draft tube in reaction turbines. However, the cavity bubbles will again collapse when coming into regions of higher pressure. These collapses produce a strong characteristic noise, and bubbles collapsing on surfaces of runner blades, runner discs, draft tube wall and so on, may damage the surfaces by a more or less terrific erodation. The whole range of turbine operation should therefore be free of cavitation. In practice that means to estimate maximum suction head.

1.1.7.2 Silt erosion

Silt erosion or Sand erosion is designated as abrasive wear. This type of wear will brake down the oxide layer on the flow guiding surfaces and partly make the surfaces uneven which may be origin also for cavitation erosion. Sand erosion therefore may be both a releasing and contributing cause for damages which are observed in power plants with a large transport of wearing contaminants in the water flow. Both the phenomenon are discussed later in detail in this work.

1.2 LITERATURE REVIEW

Single-cavity collapse in an infinite liquid was first considered by Rayleigh (1917). The model was improved by Gilmore (1957) and Hickling and Plesset (1964) performed numerical calculations under specified collapse conditions. The results show that it is possible under normal conditions to obtain very high pressures near the collapse centre, and that a spherical shock wave emitted during rebound of the cavity is attenuated approximately inversely proportional to the distance from the collapse centre. The pressure in this wave seems under typical conditions to be sufficient to cause deformation of solids if the collapse centre lies at a distance from the surface of the same magnitude as the cavity radius.

It was first suggested by Kornfeld and Suvorov (1944) that the cavities might collapse in a non-symmetrical way resulting in the formation of liquid jets. This will occur for cavities collapsing in a pressure gradient field for example produced by other cavity collapses, especially, the presence of a solid surface near the collapse centre will cause the formation of a jet directed towards the surface.

Experimental verification of this was done by Naude and Ellis (1961) and Lauterborn and Bolle (1975), and the problem was solved numerically in special cases by Plesset and Chapman (1971). If the cavity is initially in contact with the surface the jet diameter will be approximately 10% of the original cavity diameter and the jet velocity will be sufficient to enable the jet to damage the surface. However, if the cavity is initially further away from the surface the effect is greatly reduced.

Tulin (1969) has suggested that shock waves from collapsing cavities far from the surface might cause cavities near the surface to form jets of enhanced energy.

There have been several attempts to correlate the cavitation erosion resistance of a material with more well known material properties. For dimensional reasons the properties of the energy type have attracted special attention and the search has proved successful within limited types of materials. Hardness, yield strength and ultimate tensile strength have been tried, but more recently the fracture strain energy (as deduced from a tensile test) has been found to be the best single property (by for example Thiruvengadam and Waring 1966), while the ultimate resilience which is equal to the elastic work

absorbed up to fracture in tension was found to be best by Hobbs (1966), Garcia and Hammitt (1967), Hammitt et al (1969) and Hirotsu (1969).

Nevertheless Garcia et al (1966), Wood et al (1967), Robinson and Hammitt (1967) and Heymann (1969) concluded that no single energy type property could be used. Also properties with other dimensions than energy have been proposed.

Rao et al(1970) found for the case of a flow system a very good agreement between the erosion resistance and the product of either strain energy and hardness or ultimate resilience and hardness.

Tichler et al (1974) found proportionality between the erosion resistance and the true tensile strength to the 2.3 power for a limited range of materials.

Thiruvengadam et al(1969) suggest that fatigue properties should be used. It also seems obvious that the structure of the material is important as, e.g. stressed by Gould (1969).

The investigation by Feller and Kharrazi covered ten unalloyed metals and 11 alloys; three of the alloys were tested in two different heat treatment conditions. Cavitation erosion was determined by weight loss. Two sets of measurements were chosen for exploration of correlation between fatigue and cavitation erosion.

In the case of cavitation erosion in a flow system the effect of velocity has been discussed.Knapp (1955) found that the pitting was proportional to the sixth power of the velocity, and this was later confirmed in a field test by Kerr and Rosenberg (1958) and in a rotating disc apparatus by Lichtman et al (1958).

Nevertheless Hammitt (1963) found that the velocity exponent ranged from 1.7 to 4.9 depending on test conditions and Rao et al(1970) observed a variation between 6 and 25. Very few cavitation erosion rate measurements exist for flow systems, but Rao et al(1970) have found a good correlation between cavitation erosion resistance and the product of either the strain energy or the ultimate resilience and hardness.

Different analytical methods have been used to predict cavitation erosion without model tests or at least with a limited request to experiments as firstly imagined by Kato et al. (1996). Such techniques are still in development and require extensive research efforts before being operational. The models for prediction of the erosion damage applicable to ductile materials are based upon the original work done by Karimi and Leo (1987).

A few pitting and mass loss tests were conducted on an experimental device, which produces cavitation erosion from the collapse of a cavitating vortex (Dominguez-Cortazar *et al.* 1995, Filali & Michel 1999, Filali *et al.* 1999)

1.3 OBJECTIVE OF THESIS

Erosion is the main problem associated with turbines especially turbine runner which may be due to sand particles / cavitation and because of their synergetic action. Much has been done till now for combating erosion and damage under cavitational conditions by making improvements in hydraulic design and production of components, search for erosion resistant materials and arrangement of the turbines for operations within the good range of acceptable cavitation conditions. Important parameters on which inception and development of cavitation in hydro turbines depends is the turbine type and configuration, turbine setting level and turbine operation considering this , a relation or model or mathematical empirical relation is required to correlate all these parameters with cavitation erosion.

Therefore an intensive study has been carried out to understand the silt erosion and cavitation erosion, the cavitation phenomenon, silt erosion phenomenon and the erosion mechanism in detail. The objective of the present study is to find the best empirical relation for combining the parameters on which inception and development of cavitation in hydro turbines depends .The existing relations which can be satisfactorily used to determine the optimum submergence level so that the cavitation erosion is within permissible will be than verified by taking data from the actual existing site (Chilla Hydro Power Project,Rishikesh) and than estimating cavitation metal loss, efficiency loss and finally the power loss with help of another empirical equation which could further be a valuable tool in assessing a new runner design, to determine the lifetime operating cost. Extending the work theoretical optimum submergence level can be determined for a new site (Dhukwan Hydro Power Project, Jhansi) so as to keep the cavitation erosion within permissible limits .

CHAPTER -2

SILT EROSION IN HYDRO TURBINES

2.1 GENERAL

Silt erosion is a result of mechanical wear of components on account of dynamic action of silt flowing in the water coming in contact with the wearing surface. However The mechanism of erosion is complex due to interaction of several factors like sediment particles size, shape, hardness, velocity, impingement angle, concentration, properties of material and so on . The silt laden water passing through the turbine is the root cause of silt erosion of turbine components which consequently leads to a loss in efficiency thereby output, abetting of cavitation , pressure pulsations , vibrations , mechanical failures and frequent shut downs Since silt erosion damage is on account of dynamic action of silt with the component, properties of silt, mechanical properties of the component in contact with the flow and conditions of flow are therefore jointly responsible for the intensity and quantum of silt erosion. Therefore silt characteristic, velocity of silt laden water are the important factors to understand erosion intensity or extent of damage on hydro turbines.
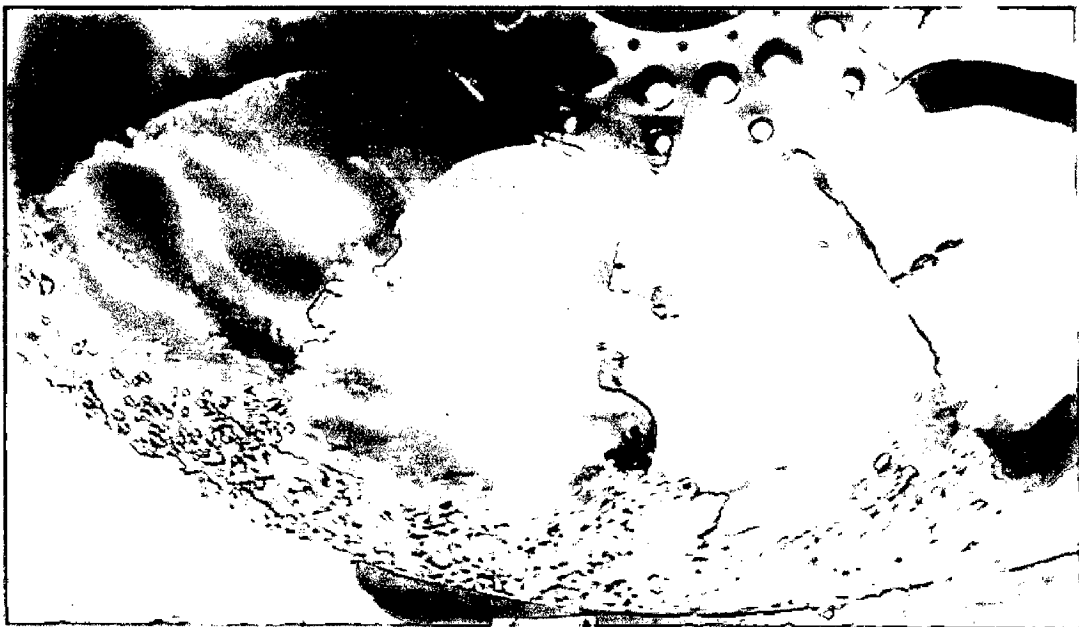
Fig 2.1 Severely damaged Kaplan runner by the impact of silt [6]

12

Fig 2.2 Silt erosion damage on the guide vanes [6]

2.2 SILT PARTICLE EROSION MECHANISM

Broadly speaking there are two abrasive erosion mechanisms according to which a silt particle can attack the target or hydro turbine[3]

1.) Gouging

2.) Hammering

Gouging is a tangential attack by the eroding body . Its action is eqivalent to the action of a tool . to resist this , the material should be as hard as possible and not allow a crack to spread.

Hammering is a normal attack by the eroding body . Its action is equivalent to a series of hammer blows . to resist this type of action , the material again has to be as hard as possible , and has to prevent the spreading of cracks.

13

Thus abrasive erosion can be considered as a combination of the two phenomena described above , with the eroding particle moving at considerable speed .

Material removal by Erosion may consist of any of the three mechanisms

1.)   Abrasion

2.)   Hammering

3.)   Impinging.

Metal removal by erosion/abrasion of various components is either by shearing-off of the metal by hard & sharp silt particles or by cracking and breaking of parent metal due to impact of the silt particles. Of the two, removal of metal by shearing-off is the major cause of erosion. . The shearing of metal can be reduced to a large extent if the particles do not hit the components at a high velocity and large angle of attack.

As it is known that silt particles attacks on the surface of the hydro turbine as a stream of solid particles so erosion of a surface by a stream of silt particles can be examined by considering the arrival times of the particles on the surface. For this treatment first a concept, an 'impact zone' is proposed, and then considers the arrival of the particles on one zone as a queuing process. The rate of erosion of ductile metals can than be predicted using simple arguments from probability theory.

2.3   FACTORS RESPONSIBLE FOR AFFECTING INTENSITY OR SILT EROSION RATE

2.3.1   Silt characteristics[4]

The physical properties of sand particles may be defined in many ways, such as grain size (equivalent diameter), shape (round or sharp edges), geological structure mainly hardness) and grading (distribution of varying sizes) and concentration .

The intensity of erosion is directly proportional to the size of the particles . particle sizes above 0.25mm are extremely harmful. It has been found that particles larger expressed in parts per million (ppm). Its cut-off values for damage to be significant are: 200 ppm for low and medium head machines (up to 150 m). and 150 ppm for high head machines than 0.25 mm, even with a hardness of less than 5 on .Moh's scale, cause wear. Similarly fine silt (less than 0.1 mm)

14

containing quartz can erode under water components. Fine silt is especially dangerous if the turbine is operating under a high head. Sharp and angular particles cause more erosion compared with rounded ones the intensity of erosion is also directly proportional to the hardness of the particles (irrespective of their size). Particles with Moh's hardness of more than 5 are harmful. Himalayan silt is 90 per cent (7 on Moh's scale compared with 10 for diamonds). The silt concentration is the most dominating factor influencing erosion intensity linearly. It is generally expressed in parts per million (ppm) . Its cut off values for damage are: 200 for low and medium head turbine (upto 150m) , and 150 ppm for high head machines .

2.3.2   Velocity of silt-laden water

The intensity of erosion is usually proportional to the cube of the velocity V of the water carrying silt particles in suspension. This is particularly true for Francis runners. Any decrease in velocity, therefore would substantially reduce erosion damage. For instance, a 10 per cent decrease in water velocity could reduce erosion by 27 per cent.

2.3.3   Machine flow pattern[4]

Intensity of silt abrasion is closely related to the local flow pattern in a machine i.e. same specimen materials can suffer different degrees of damage when placed in different locations with different types of flow. On the other hand, same type of abrasion can occur for each kind of material when placed at different locations, but with the same type of flow pattern.

2.3.4   Power Plant design criteria[5]

Intensity damage due to silt at different power stations may vary even where silt conditions are identical which cleary indicates that equipment design has a significant role to play in influencing the intensity of erosion . Power plant design necessarily includes water passage, rotation speed and number of runner blades etc .

When a turbine is designed to handle high concentrations of silt, selection of a conservative specific speed is advisable. The adverse effect of silt is reduced in oversized machines. The rotation speed should be lower than the synchronous speed selected for a machine to be used in clean water. Experience also shows that design optimization is possible to mitigate silt erosion of critical zones. From the basic principles of hydrodynamics, the energy transfer by hydrofoils

results from their angle of incidence, curvature and shape. These parameters create differential velocities over the blade surface, and the rate of change of velocity depends on the curvature and length of the blade. It has been found that the peak velocity can be moderated by increasing the blade length, and the wearing life can be increased by increasing the thickness of the blades, especially towards the tip section. The turbine runner needs to be designed taking account of the following boundary conditions:

- minimum curvature of the blade profiles towards the tip in the case of Kaplan units, and towards the outlet edge nearer the skirt in the case of Francis machines;

- point of maximum curvature as near as possible to the inlet edge in the case of Francis units and near to the hub in the case of Kaplan units, as well as reduction of curvature towards the outlet edge in both cases;

- minimum angle of incidence;

- long blade profiles and a flat rear section;

- minimum number of blades; and,

- blade profiles to be as thick as possible with appropriate thickness distribution.

2.3.5 Wear resistance of material

2.4 SILT EROSION RATE

By combining the above factors Silt erosion rate (W) can be expressed mathematically as[6]

$$W \propto C_1 C_2 C_3 C_4 M_r V^x$$

C_1 = Coefficient of silt concentration;

C_2 = Coefficient silt hardness;

C_3 = Coefficient of silt particle;

C_4 = Coefficient of silt particle shape;

Mr = coefficient of wear resistance of base material; and

V = velocity of water.

The following values of the exponent x are suggested:

3 for Francis runners; 2.5 for vanes and pivot ring liners; 2.5 for Pelton nozzles and 1.5 for Pelton runner buckets

2.5   ABRASION CRITERION FOR HYDRAULIC TURBINES[4]

The product of operating head H and content of harmful sediments S_d (d>0.05mm) that essentially represents the energy content of the particles is selected as a measure of abrasion intensity. $HS_d = 7$ is roughly the dividing line between moderate damage and serious damage.

2.6   TURBINE EFFICIENCY IN SILTY WATER [5]

It is important for new machine designs to undergo appropriate model testing with silty water to determine efficiency. The turbine efficiency is extremely sensitive to increased clearances between the guide vanes and their holding rings, besides runner labyrinth clearances. Even before any wear has taken place, the overall efficiency in silty water is reduced in proportion to the solids content.

Hydraulic performance tests on a Francis turbine model with sediment- laden flow, conducted in Japan, showed that the turbine's best efficiency decreased

almost in direct proportion to the increase in solids concentration or the specific gravity.

The reduction in peak efficiency (η) is expressed[5] as:

$\eta_m = (1 - 0.085\ C_w)\ \eta_w$

η_m = turbine peak η with sediment laden flow (mixture);

η_w = turbine peak η with clean water; and,

C_w = fraction of solids by weight.

The critical cavitation coefficient was also found to be influenced by the presence of silt in the flow; it increases in direct proportion to the mixture concentration at each unit speed .

2.7   THEORIES FOR EROSION MECHANISM [7]

To understand the the mechanism of erosion on hydro turbines by silt particles we can take help of the various mechanistic theories developed for the material removal when a ductile metal target is eroded by solid particles (usually harder than the target) which are described as follows.

(i) Erosion by cutting: Finnie (1958), Hutchings (1977), Hutchings *et al* (1976),

(ii) Erosion by deformation wear: Bitter (1963a, b).

(iii) Erosion by target melting: Neilson and Gilchrist (1968), Smeltzer *et af* (1970),

(iv) Erosion by delamination wear: Suh (1973), Jahanmir (1980).

- Erosion by cutting has been observed using high-speed photography by Hutchings (1977); it is the result of a sharp cornered projectile machining a chip of material from the target surface. Each impact leading to the removal of a chip is considered to be independent and the total amount of erosion is the sum of the contributions from each micromachining impact. This theory, which evolved from the study of the machining process on lathes, is both quantitatively and qualitatively successful. However, not all eroding particles are angular and not all impacts give rise to detached chips of material and therefore this theory appears to be unable to deal with these exceptions.

- When a projectile impinges upon the surface of a ductile target it loses some kinetic energy. Most of this lost energy is transformed into plastic deformation and then into heat within the target.If this heat is generated sufficiently quickly and within a small enough volume of the target then the temperature there can reach the melting point. Target material can then be removed more easily due to its much reduced cohesive strength.

    Qualitative observations which indicate that melting has occurred have been restricted to scanning electron microscopy of eroded target surfaces (Smeltzer et aZ1970, Shewmon 1979). This kind of evidence cannot be accepted as proving that melting is a dominant mechanism of erosion. In support of the theory Neilson and Gilchrist (1968) and Uetz and Gommel (1966) have measured a rise in the temperature of a target during erosion. Clearly erosion by melting can be either a cooperative or an independent effect of the eroding projectiles. Independent melting will occur if every impact releases sufficient heat energy to cause spontaneous melting, However, cooperative melting can still occur if the energy released per impact is insufficient to cause spontaneous melting.

- Suh's (1973) theory of abrasion by delamination wear has been extended by Jahanmir (1980) to include erosion. The target is considered to be composed of a matrix containing harder inclusions The projectile interacts with the surface by sliding across it but not directly removing material. Delamination can only occur when

subsurface cracks start to extend parallel to the target surface. These cracks are nucleated by voids which can form at the interface between the matrix and the inclusions. In order to nucleate a void, there must be present around an inclusion both a large shear stress and a large hydrostatic stress. This latter stress is not present initially. However, repeated sliding across the same portion of the target surface apparently gives rise to large residual stresses and these are considered to be the source of the hydrostatic stresses. Clearly, the mechanism of delamination is a cooperative effect.

- Bitter (1963a, b) assumed that the removal of material from the surface of a target occurs by the joint action of two mechanisms: cutting, which only occurs when the projectile strikes the target at grazing incidence; and deformation wear, which predominates at normal impingement. Unfortunately he did not explain clearly how material was removed by deformation wear. It may be that it is low-cycle fatigue (Hutchings 1979) or, indeed, delamination wears. However, Jahanmir (1980) discusses delamination in terms of a projectile sliding across a surface and sliding is impossible at normal impingement.

Bitter (1963a, b) was careful to point out that deformation wear is characterized by repeated bombardment, by which he implies that it is a cooperative mechanism.

None of these theories is capable of explaining all of the effects normally observed in erosion experiments. Two effects, which remain largely unexplained, are the influence of the duration and magnitude of the eroding flux on the amount of erosion.

Numerous authors (Tilly 1969, 1970, Uuemois and Kleis 1975) have observed a time delay before the commencement of loss of mass from an eroded target. Fig 2.3 depicts typical erosion behaviour involving a time delay or incubation time.

Figure 2.3(a) (from Tilly 1969) is a graph of mass loss from a target against duration of testing. The incubation time is apparent as a period during which the target has increased in mass. This is commonly associated with particles embedding in the target surface which will be discussed at a later stage. Figure 2.3(b) (from Uuemois and Kleis 1975) is a graph of what the authors call 'erosion rate' against duration of testing. It is obtained from mass loss data. The total mass loss M within a time t is related to the 'erosion rate' (or more precisely

the relative erosion), W, by the ratio of $M/G = W$, where G is the mass of eroding particles which has struck the target within the same time period t. The term 'erosion rate' is sometimes associated with a definition in the form of an instantaneous time derivative. Many data have already been given in which 'erosion rate' is defined as $W=M/G$ and the same definition is used here.

2.8   ANALYSIS OF SILT PARTICLE MECHANISM

F is the erosive flux; it is the silt mass rate crossing unit area of orifice. Throughout this work it will be assumed that F is constant. Clearly, $G\ \alpha\ Ft$ and $W\ \alpha\ M/t$. The erosion rate is not by definition equal to the time derivative of the mass loss (dM/dt) but if the loss of mass was to increase linearly from t $=O$ then dM/dt=M/t and the erosion rate graph would become a straight line parallel to the time axis. Figure Ia indicates that this behaviour is obtained but only after the incubation period has passed,

Unfortunately, Uuemois and Kleis (1975) do not indicate what form Fig 2.3(b) takes at short times. Experimental errors are relatively large at short times when the mass losses are smallest and it is common to see this portion of the curve omitted. The curves in figures 2.3(a) and *(b)* were both obtained from experiments performed at constant flux, In the discussion that follows models are presented which generate mass loss curves. The complementary erosion rate is as calculated and both curves are plotted which will give the shape of the curve as shown in graph. Examining theoretically the influence of time and flux on the loss of mass from a target with to the primary mechanisms. The concept of 'impact zone' associated with the impact of a single projectile is used and following this, there is a discussion of the queuing theory for the arrival of projectiles on one impact zone.
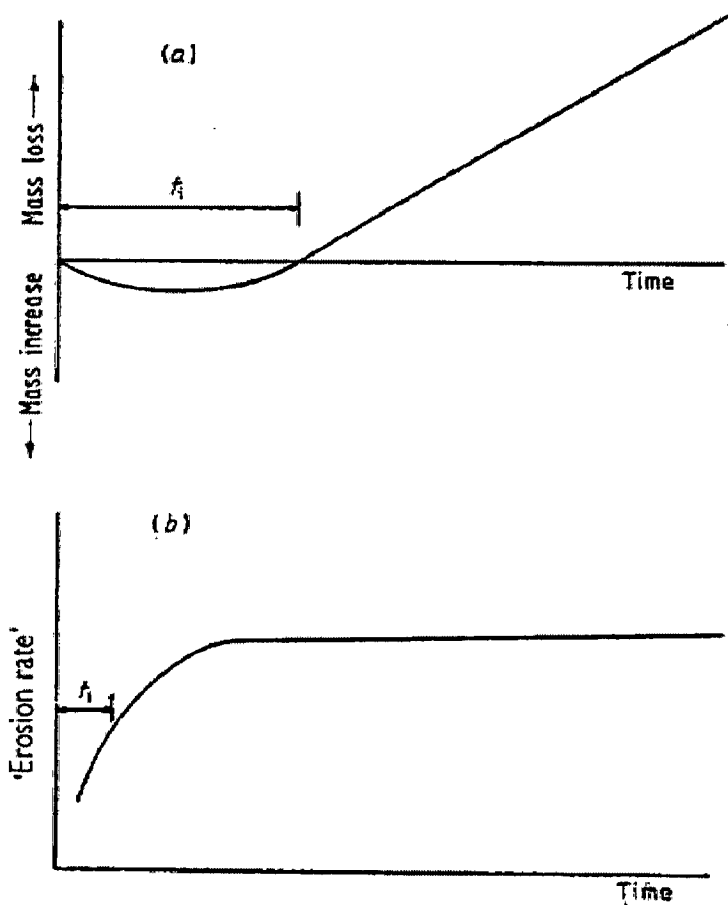
Figure 2.3. *(U)* Change of mass of an eroded target with the duration of the test (typical behaviour). After an initial period of incubation t_i a linearly increasing mass loss is established (after Tilly 1969). *(b)* Variation of 'erosion rate' (relative erosion) with time of test for a metal target (typical behaviour). The plateau region is an indication that a constant rate of erosion has been established. (After Uuemois and Kleis 1975.)[7]

2.8.1 Concept of impact zone[7]

The impact zone is the zone of plastic deformation around an impact site. If a precise measure of the zone size is required, it is best measured rather than estimated. This can be done by firing only a few particles at a virgin target surface so that there is little chance of zones overlapping. The procedure which follows averages over many zones so that the error resulting from variation of the size of the impact zones becomes unimportant.

The impact zones are also considered to be non-interacting; erosion occurring on one zone does not influence the rate at which material is removed from adjacent zones. All zones are

considered to be identical and edge effects are neglected. The datum point for time is taken as the commencement of the erosion test.

The average number of particles per second striking one zone, Ω, (the zone impact frequency) equals $F\sigma/m$. However, if the arrival of particles is random then the probability of an impact occurring inside some small time interval (t_1, $t_1+\delta t$) is simply $\Omega\delta t$. This probability is unaffected by the pattern of events before time t_1. If δt is chosen to be small (i.e. $\delta t < 1/\Omega$) then the probability that two or more impacts will occur within (t_1, $t_1+ \delta t$) is negligible. As these are the conditions of a Poisson process, it follows that the arrival of projectiles on to an impact zone is described by the Poisson distribution,[7]

$$P(r) = \left[(\Omega t)^r / r! \right] \exp(-\Omega t)$$

r = number of impacts in(0,t).

The mean μ of the Poisson distribution is a standard result:

$$\mu = \Omega t$$

To calculate the loss of mass from one impact zone in the time interval (0, t) it is necessary to equate the loss of mass to the number of particles striking one zone during that interval. It is at this point that any cooperative effect of the impacts of projectiles becomes important.Using the above equation it is straightforward to calculate the expected mass loss from one zone (and hence from the whole target) using one linking mass loss equation.

2.8.2 Mass loss equations [7]

Each impact is treated as an independent event and it is assumed that every impact removes the same (average) mass, m_c, of material from a zone. Expected mass loss, M_z from one zone in (0, t)

$$M_z = m_c \sum_{r=0}^{\infty} r[(\Omega t)^r / r!] \exp(-\Omega t)$$

The equation can be simplified to give

$$M_z = m_c \Omega t$$

Multiplying by the number of impact zones on the target, the expected mass loss, M, from the whole target in time (0, t) becomes

$$M = (A/\sigma)\, m_c \Omega t$$

Or in terms of the total flux F

$$M = FA(m_c/m) \; t$$

The erosion rate W associated with the mass loss can be found by dividing by the total mass of particles striking the target in time t (i.e. *FAt*).

$$W = M/Fat = m_c/m = constt$$

This model describes the erosion characteristic of a process involving only independent impacts. Into this category fall the cutting mechanism and the independent melting mechanism of erosion.

To improve this further the impacts are considered not be independent and it is assumed that the loss of mass from a zone cannot commence until the number of impacts exceeds a value which depends on time.

Now the expected mass loss from the target

$$M = \frac{A}{\sigma} m_m \sum_{r=r'}^{\infty} (r - r') [(\Omega t)^r / r!] \exp(-\Omega t)$$

and the rate of erosion can be given by

$$W = \frac{m_m}{F\sigma t} \sum_{r=r'}^{\infty} (r - r') [(\Omega t)^r / r!] \exp(-\Omega t)$$

Cooperative melting requires that heat is generated in the surface of the target at a sufficient rate to raise the target temperature to the melting point and to maintain it at this level. *

Thus by using the idea of an impact zone it is possible to treat statistically the arrival of particles on the surface of the target. It is not only easier to visualize erosion on one impact zone it is also straightforward to determine the loss of mass from that zone using simple probability theory.

2.9   SILT EROSION / CAVITATION SYNERGY

As mentioned earlier, the extent of material removal depends on the velocity and force with which the particles act over the surface if blade curvature is relatively high, the resulting higher centrifugal force on the particles increases the intensity of erosion. Over a period of

operation in silty water the surface becomes irregular, which, in turn induces local cavitation. Subsequently. the destruction is faster as a result of the combined effects a turbine component completely free from cavitation when operating in clean water is affected by cavitation in silty water. Furthermore, a component already eroded by silt erosion is much more prone to cavitation pitting. The combined effect can be very severe and can be understood as follows

With the hydraulic design parameters adopted these days (high specific speed), cavitation is considered to be largely responsible for the initiation of damage. Generally, removal of metal from a runner (excluding other underwater parts), is limited to 0.1 D^2 kg per 1000 h of operation, where D is the throat diameter of the runner in meters. For the sake of economy in manufacturing costs of turbines and generators, manufacturers do permit limited cavitation to take place. Turbine settings are thus fixed by the manufacturers, so that cavitation remains within the guaranteed limits. Some restrictions on operating conditions are also imposed. The above is generally based on the assumption that turbines will be operated in fairly clear water and thus no major damage is expected.

When cavitation does take place, the affected area develops pumiceous and honeycomb like pits, and the metal is weakened. Because of this, the water flow is locally disturbed. If the water is clean, there is generally no serious problem as a result of this limited cavitation. However, when silt-laden water passes over this, the spongy area is rapidly removed as a result of sliding abrasion. The fresh runner area develops a similar pumiceous spongy surface (from cavitation) and is again removed by the grinding action of the sand, which is present in the water. The rate of removal depends on the size, hardness, roughness, silt concentration and velocity of the water. Thus, the outlet edges of the turbine blades, where velocities are higher, become thinner. Vibration takes place and, as a result of fatigue, cracks develop and ultimately, pieces of the runner wash out. The lost pieces of the runner blade greatly disturb the flow condition, and severe damage occurs.

If the turbines operate in clear water, it takes a much longer time for the water to remove the cavitation-affected spongy areas. The presence of silt accelerates the damage. The damage caused by a combination of cavitation and abrasion is therefore much more rapid and severe compared with damage caused by either of them separately.

Some well-known facts about cavitation erosion and sand abrasion are:

➢   The viscosity of particle-laden flow is higher than clear water, especially when the water

contains very fine grains such as ash and clay. As the critical vapourizing pressure is raised, the inception of cavitation is delayed.

➤ The intensity of cavitation erosion is related to the velocity of the flow in the sixth power or higher. .

➤ The intensity of sand erosion is roughly proportional to the third power of flow velocity.

➤ There is an evident incubation period with cavitation erosion. The rate of damage may be identified with stages of incubation, acceleration, deceleration and equilibrium. Sand erosion has no incubation period damage is simply proportional to time.

Damage to metal surfaces where there is interaction between cavitation and erosion is much more serious than each attack alone.

CHAPTER -3

CAVITATION EROSION IN HYDRO TURBINES

3.1 GENERAL

Cavitation consists of evaporation and condensation of a liquid. Cavitation normally occurs when liquid at constant temperature is subjected to vapour pressure. In fluid power applications the evaporation pressure is reached when flow velocity is increased sufficiently. The occurrence of cavitation in fluid power is mostly detrimental. One of the devastating consequences of cavitation is the mechanical degradation of a solid material(cavitation erosion).

Cavitation affects fluid power systems and components in various ways, which are usually undesirable. For example efficiency of a system is reduced due to cavitation and vibrations as well as noise level of a system is increased. One of the remarkable consequences of cavitation is cavitation erosion. Cavitation erosion is formed when cavitation is violent enough and occurs close to adjacent material surfaces. Cavitation erosion is always very harmful as it causes fluid contamination, leakage, blockages and undesired operation of system.

3.2 CAVITATION PHENOMENON

3.2.1 Definition

Cavitation is defined by Knapp et al[10] as the condition when a liquid reaches a state at which vapour cavities are formed and grow due to dynamic-pressure reductions to the vapour pressure of the liquid at constant temperature. In a flowing liquid, these cavities are subjected to a pressure increase that stops and reverses their growth, collapsing implosively and disappearing. The violent process of cavity collapse takes place in a very short time of about several nanoseconds and results in the emission of large amplitude shock-waves, as demonstrated by Avellan and Farhat. A high-speed reentrant liquid micro-jet directed towards the boundary can also occur for cavities collapsing close to a solid surface. If the amplitude of the resulting pressure pulse is larger than the limit of the material mechanical strength, a hollow or indentation of several micrometers called "pit" will be formed on the surface. If an accumulation of pits takes place in a narrow area, the material is finally eroded and mass loss occurs due to the repetitive action of the

cavity collapses. In a flowing liquid, these cavities can take different forms that can be described as travelling bubbles, attached cavities or cavitating vortices.

In general Cavitation is a term used to describe a process, which includes nucleation, growth and implosion of vapour or gas filled cavities. These cavities are formed into a liquid when the static pressure of the liquid for one reason or another is reduced below the vapour pressure of the liquid in current temperature. When cavities are carried to higher-pressure region they implode violently and very high pressures can occur.[11] When the local pressure of a liquid is reduced sufficiently dissolved air in oil starts to come out of solution. In this process, air diffuses through cavity wall into the cavity. When pressure in the liquid is further reduced, evaporation pressure of the liquid is achieved. At this point the liquid starts to evaporate and cavities start to fill with vapour. When this kind of a cavity is subjected to a pressure rise cavity growth is stopped and once the pressure gets higher cavities start to diminish. Cavities disappear due to dissolution of air and condensation of vapour. When a cavity is mostly vapour filled and subjected to a very rapid pressure rise it implodes violently and causes very high pressure peaks. Implosion is less violent if the gas quantity of a cavity is great which requires relatively slow nucleation of a cavity.
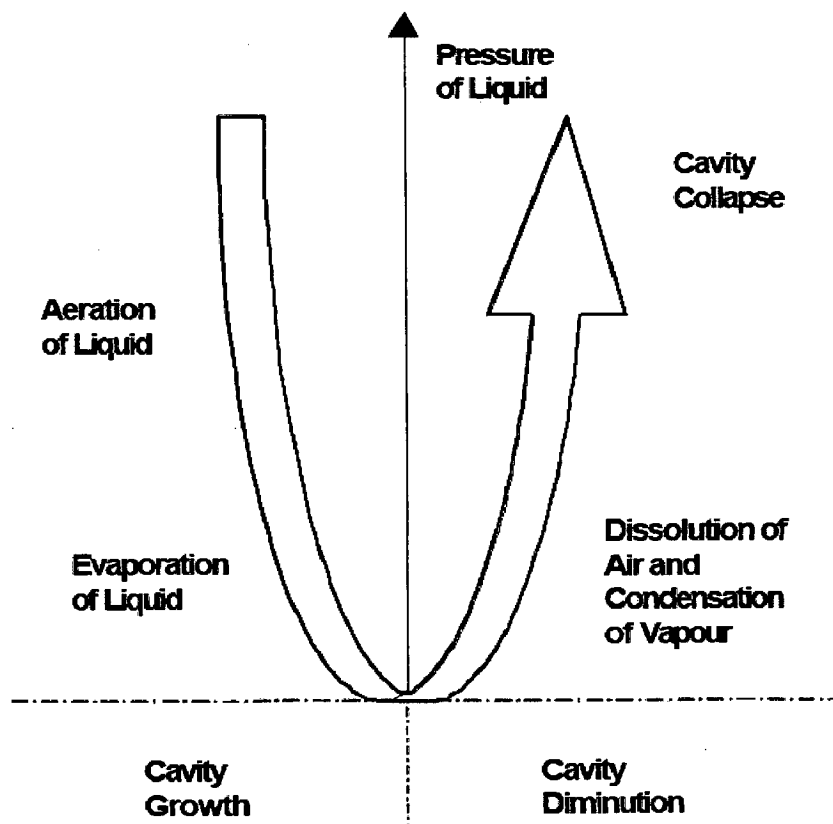
Fig 3.1 Cavitation process[11]

3.2.2 Travelling bubbles

Bubbles usually appear around a body from micron-sized nuclei in low-pressure regions of the flow (see left of Fig3.2). Travelling with the flow, they implode when they find an adverse pressure gradient. These bubbles are strongly influenced by the air content of the liquid. Nevertheless, their erosive power is considered to be relatively weak.

3.2.3 Attached cavities

Cavitation can take the form of macro-cavities that develop an attach on a solid wall placed in the flow. For instance, the so-called partial cavitation grows from the leading edge on the suction side of a hydrofoil with a positive angle of incidence. This is a very common and complex type of cavitation that can present different regimes depending on the hydrodynamic conditions. One of the regimes, sheet cavitation, is characterised by thin stable cavities with smooth and transparent interfaces. At their rear part, the cavity closure presents a slight and weak pulsation due to the shedding of small cavitation vortices so that it represents a low risk of erosion. Another regime, cloud cavitation, shows a strong unsteadiness and a pulsating behaviour that provokes significant oscillations of the cavity length (see centre of Fig.3.2). The cavity interface is wavy and turbulent. Large U-shaped transient cavities and clouds of cavities are shed away downstream of the cavity closure that collapse violently on the solid surface. Consequently, this is a very aggressive form of cavitation with a high erosive power. When this type of cavitation occurs in turbomachinery it can induce abnormal dynamic behaviour and cause serious erosion.
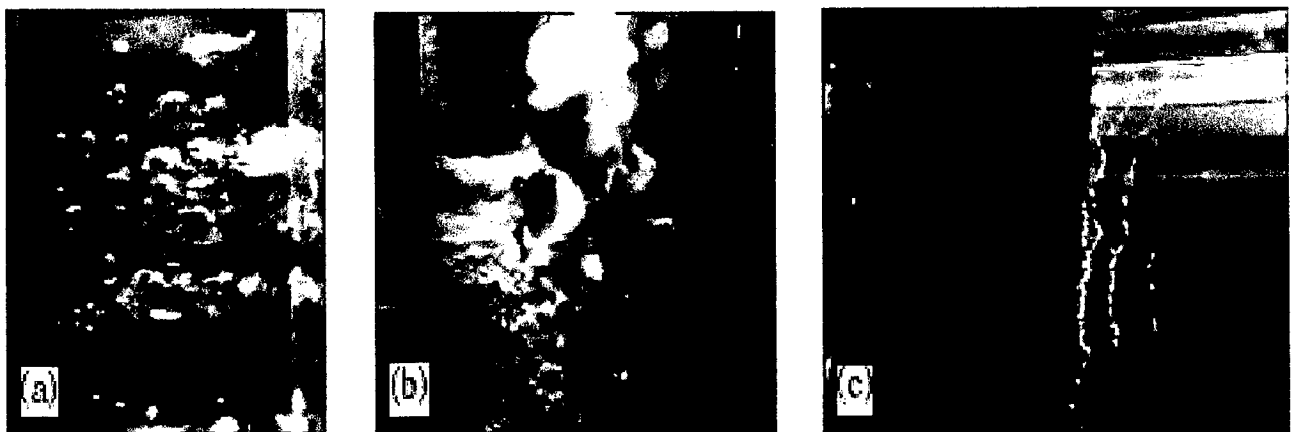
Fig3.2 Types of cavitation on a 2D hydrofoil(flow from left to right):(a)travelling bubbles, (b)unstable attached sheet and (c) Von Karman vortex-shedding.[10]

3.2.4 Vortex cavitation

Flow regions with concentrated vorticity can develop cavitation in their central cores due to the low pressures generated. If the tips of these vapour filled vortices are in contact with a solid surface they become potentially erosive since the final collapse of the whole cavity takes place on them. A typical example of this type of cavitation can develop if Von Karman vortex shedding occurs at the trailing edge of a hydrofoil and pressure is low enough (see right of Fig3.2). As a result, lift fluctuations are provoked synchronised with the shedding frequency. Vortex cavitation can also occur in the flow channels of hydraulic machines when they operate at part load. In the case of a coupling phenomenon with a natural frequency this can lead to fatigue damage.

3.3   MAIN TYPES OF CAVITATION

3.3.1 Leading edge cavitation

Leading edge cavitation takes the form of an attached cavity on the suction side of the runner blades due to operation at a higher head than the machine design head when the incidence angle of the inlet flow is positive and largely deviated from the design value It can also occur on the pressure side during operation at a lower head than the machine design head when the incidence angle is negative. If unstable, this is a very aggressive type of cavitation that is likely to deeply erode the blades and to provoke pressure fluctuations.

3.3.2   Travelling bubble cavitation

Travelling bubble cavitation takes the form of separated bubbles attached to the blade suction side near the mid-chord next to the trailing edge. These travelling bubbles appear due to a low plant cavitation number and they grow with load reaching their maximum when the machine operates in overload condition with the highest flow rate This is a severe and noisy type of cavitation that reduces significantly the machine efficiency and that can provoke erosion if the bubbles collapse on the blade.

3.3.3   Draft tube swirl

It is a cavitation vortex-core flow that is formed just below the runner cone in the centre of the draft tube. Its volume depends on cavitation number and it appears at partial load and at

overload due to the residual circumferential velocity component of the flow discharged from the runner. This vortex rotates in the same direction as the runner at part load and in the opposite direction at overload. From 50% up to 80% of the best efficiency flow rate, the vortex core takes a helical shape and presents a precession rotation at 0.25–0.35 times the runner rotating speed. In this case, circumferential pressure pulsations are generated at this low frequency. Strong fluctuations may occur if the precession frequency matches one of the free natural oscillation frequencies of the draft tube or penstock. This provokes large bursts of pressure pulses in the draft tube causing strong vibrations on the turbine and even on the powerhouse. Beyond the best efficiency point the vortex is axially centred in the draft tube cone.

3.3.4 Inter – blade vortex cavitation

This is formed by secondary vortices located in the channels between blades that arise due to the flow separation provoked by the incidence variation from the hub to the band. They can attach to the intersection of the blade inlet-edge with the crown or mid-way of the crown between the blades close to the suction side. Only if their tip is in touch with the runner surface they can result in erosion. These vortices appear at partial load operation and yield a high broadband noise level. They can also appear and cavitate at extremely high-head operation ranges because the cavitation number is relatively low. In this case, they become unstable and cause strong vibrations.

3.3.5 Von Karman vortex cavitation

From the trailing edge of blades and vanes periodic vortex-shedding can occur. Severe pulsations and singing noise can be caused if a lock-in phenomenon occurs. As a result, the trailing edge might be damaged.

For Kaplan turbines, leading edge cavitation is less likely to occur than in Francis turbines. This is because the runner blades have a variable pitch and the machine always operates in "on cam" condition. This means that α(angle of incidence) is close to the optimum value over a wide operating range thanks to the good combination between runner blade inlet angle and guide vane angle. For the same reason, draft tube swirl is also less severe than in Francis turbines. Travelling bubble cavitation can take place too on the blades suction side due to heavy blade loading. An exclusive type of cavitation of Kaplan turbines is tip vortex cavitation. This cavitation arises in the gap or clearance between the blade tip and the casing. It is a strong type of cavitation that damages

an area along the mid-chord length on the periphery of the blade suction side because the vortex tip touches the blade surface. The area on the blade tip end can also suffer erosion[12].
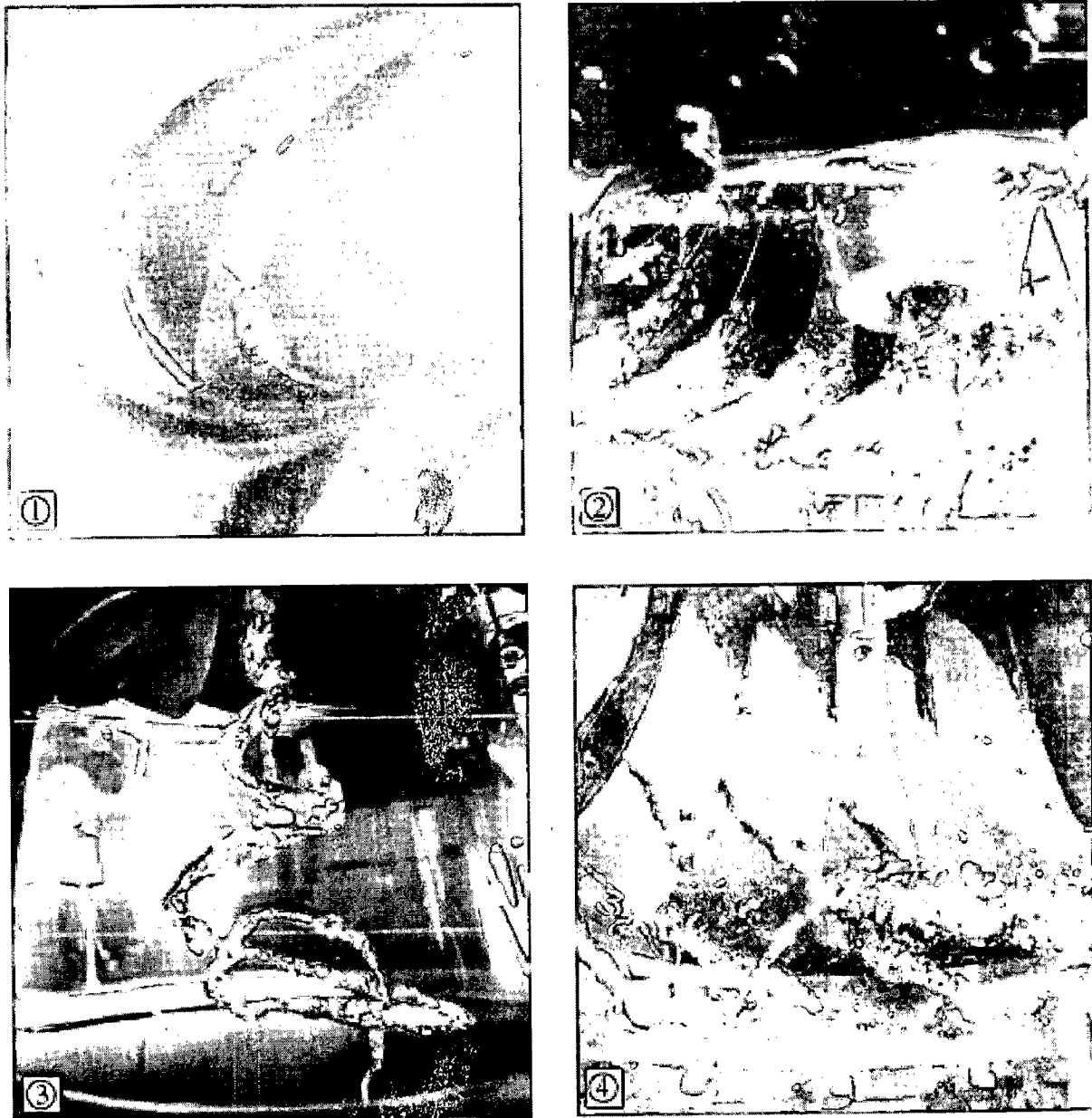
Fig3.3 : (1) leading edge cavitation, (2) travelling bubble cavitation, (3) draft tube swirl and (4) inter-blade vortex cavitation. Pictures 1 and 4 courtesy of Franc et al.Picture 2 courtesy of Grindoz[10]

3.4 CAVITATION EROSION

Mechanical degradation of a solid material caused by cavitation is called cavitation erosion. Cavitation erosion can be formed when cavity implosions are violent enough and they take place near enough to the solid material. Cavitation erosion can be identified from a specific rough mark in surfaces of component flow paths. Despite the great deal of research the actual mechanism of cavitation erosion is still not fully clear. At present it is considered that there are two possible mechanisms to cause cavitation erosion. When a cavity collapses within the body of liquid, the collapse is symmetrical. The symmetrical collapse of a cavity emits a shock wave to the surrounding liquid (see Fig 3.4). When a cavity is in contact with or very close to the solid boundary, the collapse is asymmetrical.

In asymmetrical collapse the cavity is perturbed from the side away from the solid boundary and finally the fluid is penetrating through the cavity and a micro-jet is formed (see Fig3.4). However, it has been stated [Hansson and Hansson (1992), Preece (1979)] that each of these mechanisms has features that do not give a full explanation to the observed cavitation erosin phenomena. The shock wave is attenuated too rapidly and the radius of the cavity micro-jet is too small to produce the degree of the overall cavitation erosion. Nevertheless, when a cloud of cavities collapses, the cavities do not act independently, but in concert (triggering each other's collapse). The collapse of the cavity cloud enhances the effects of the cavities adjacent to or in contact with the solid boundary.

Although it is supposed that the material is eroded under the action of collapsing cavities in the following way.

(a) At first the cavitation results in a heavily deformed surface on a macro level (the order of magnitude of the initial cavity diameter). This goes on practically without mass loss as long as the material is not fully work-hardened.

(b) Secondly the mass loss period starts resulting in formation of new surfaces. The mass loss may arise for example from the formation of cracks in and below the surface or by the formation of lips which then break off .

However the degree of cavitation erosion is affected by various factors. The intensity of cavitation determines the load, which is subjected to a solid surface. Geometry of flow paths, pressure distribution in a system, and properties of fluid, including cleanliness level of the fluid determine the intensity of cavitation. The solid material itself does not affect the existence of

cavitation. When cavitation exists, the formed cavitation erosion is dependent on material properties like hardness, work hardening capability, and grain size. Also stress state and corrosion resistance of a material affect the degree of cavitation erosion.
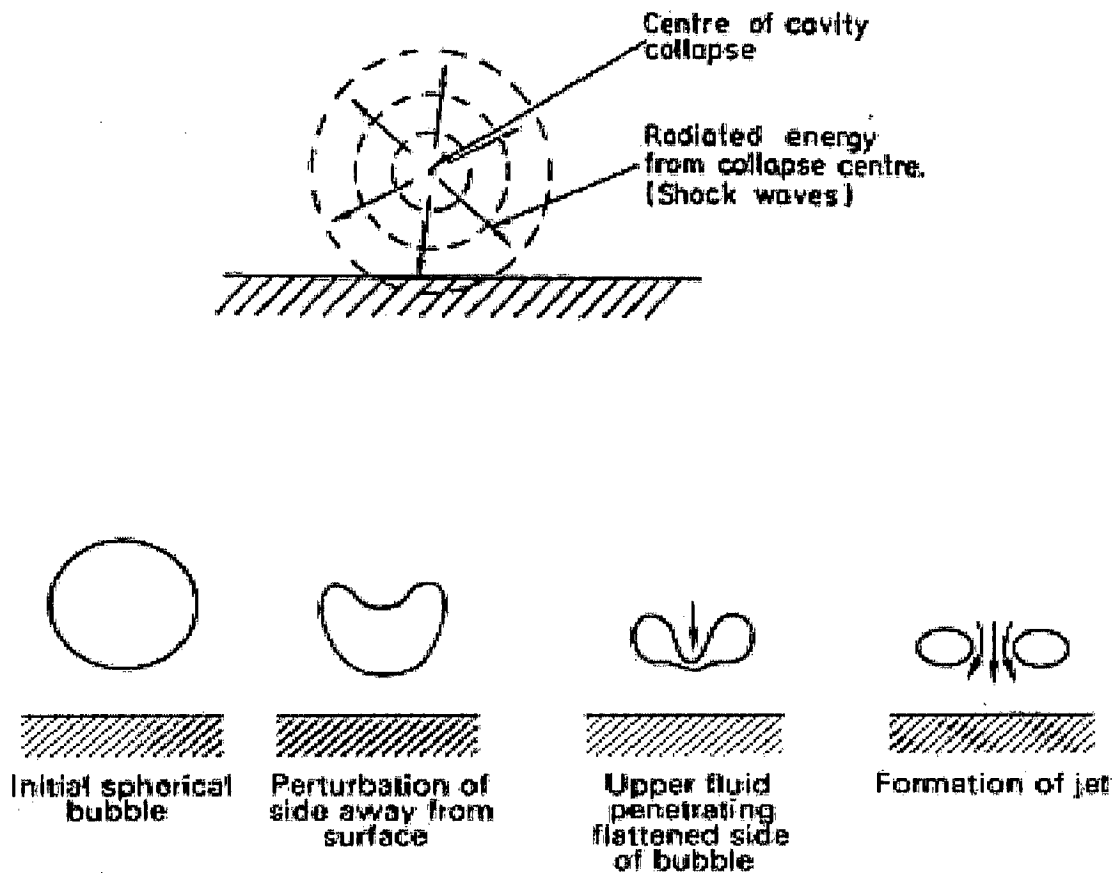
Fig 3.4 The shock-wave mechanism and micro-jet mechanism of cavitation erosion.

[Lamb (1987), Knapp et al. (1970)][11]

3.5 UNDERSTANDING CAVITATION IN KAPLAN TURBINE

3.5.1 Cavitation starting at the blade leading edge

Attached sheet cavities starting at the leading edge are usually the result of a mismatched angle of attack, causing a flow separation close to the leading edge. At this particular runner, two attached sheet cavities were usually found, one small and one large, at the leading edge on the suction side. Although the sheet cavities are near each other, they are more or less detached from each other depending on the running condition. The small sheet cavity is located closer to the hub, whereas the large sheet cavity is located further out. Both cavities have convex closure ends and are

33

relatively stable with minor volume fluctuations, however the surface of the small sheet cavity is much more disturbed than that of the large one.

The distorted cavity interface in the closure region is linked with a disintegration of the sheet into small parts which are convected downstream. The disintegrated voids can be characterized as cavitating bubble clouds, vortex cavities of horse shoe shape (also called ring vortex, hairpin-shaped vortex and inverse Unshaped vortex) or long stream oriented cavitating vortices (see photographs in Fig3.5)[12].
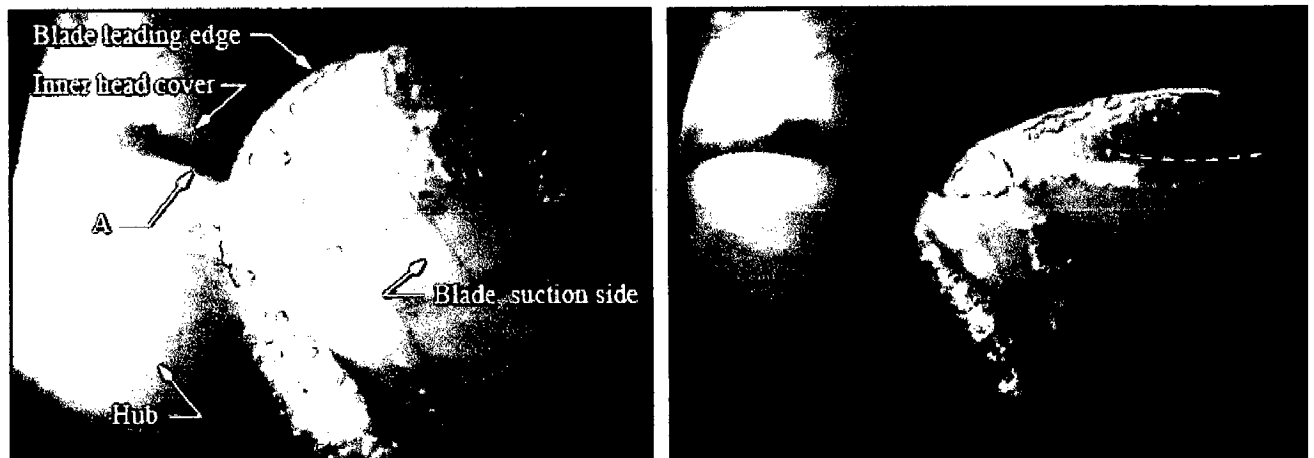
(a) Small attached sheet cavity at the leading edge, closer to the hub, and a large sheet cavity further outwards towards the blade periphery. The surface of the small sheet cavity is more disturbed than the surface of the large one. Cavitation originating from the join between the rotating Hub and the stationary inner head cover as shown at A

(b) Relatively large cavitating ring vortices broken off from the small attached sheet cavity fairly regularly. The cavitating vortices are approximately of the same size as the sheet cavity from which they originate.The trace of the reentrant jet front in the large sheet cavity has been marked with a white dashed curve .

Fig 3.5 : The sheet cavities have convex closure ends and disturbed surfaces

cavitation at the leading edge of the blade is cavitating ring vortices which are broken off from the closure end of the sheet cavities, after which they are convected downstream with the vortex ends against the blade surface. Since the vortices are convected downstream with the vortex ends touching the blade surface, the collapse occurs very close to the blade surface, which is a basic requirement for erosion

The ring vortices are usually broken off at the convex closure region of a sheet cavity and are of approximately the same size as the convex part of the cavity.

3.5.2 Cavitation at the blade root

Cavitation at the blade root appears as two different types of cavitation (see Figure 3.6(a) and 3.6(b)).The type of cavity that appears depends on the running condition. The travelling bubble cavitation shifts towards sheet cavitation as the bubble concentration is increased by decreasing the cavitation number.

The root cavities appears at two locations, one is located close to the blade flange on the blade surface (inner root cavity), while the other is located further out on the blade surface. The latter has a shape resembling a cavitating vortex. The inner cavity,on the other hand, shows no signs of any rotation: it can be either of travelling bubble or of sheet type.

Some flow mechanisms influencing the cavitation at the blade root were found to originate from the following places:

a) The fillet between the blade and the blade flange at the upstream end of the flange (A in Figure 3.6(c));

b) The corner between the blade leading edge and the hub (B in Figure 3.6(c)); and

c) The join between the rotating hub and the stationary inner head cover (C in Figure 3.6(c))

Flow disturbance from the upstream end of the blade flange fillet (Mechanism a) The cavitation that originates from point A in Figure 3.6(c) and is located close to the blade flange fillet is called the inner root cavity. Figure 3.6(a) shows an example of it at a incipient stage, appearing as travelling bubble cavitation.

A primary reason for cavitation in the region of the blade flange fillet is a decrease of pressure caused by the body shape at the fillet. There may also be a contribution caused by a mixing of two boundary layers, i.e. the blade boundary layer and the hub boundary layer. Perhaps the mixing process causes a flow separation and, consequently, a low-pressure area where the inner root cavity is located. The blade boundary layer is initiated at the blade leading edge, whereas the hub boundary layer is initiated much further upstream. Under conditions of moderate cavitation development, as in Figure 3.6(a), bubbles are initiated at the fillet, whereupon they are convected downstream while expanding. With a somewhat higher concentration of bubbles (lowered cavitation number or altered running condition) the growth process remains the same, but the bubbles will then merge together more with neighbouring bubbles before collapsing. The collapse is sometimes followed by minor rebounds[12].
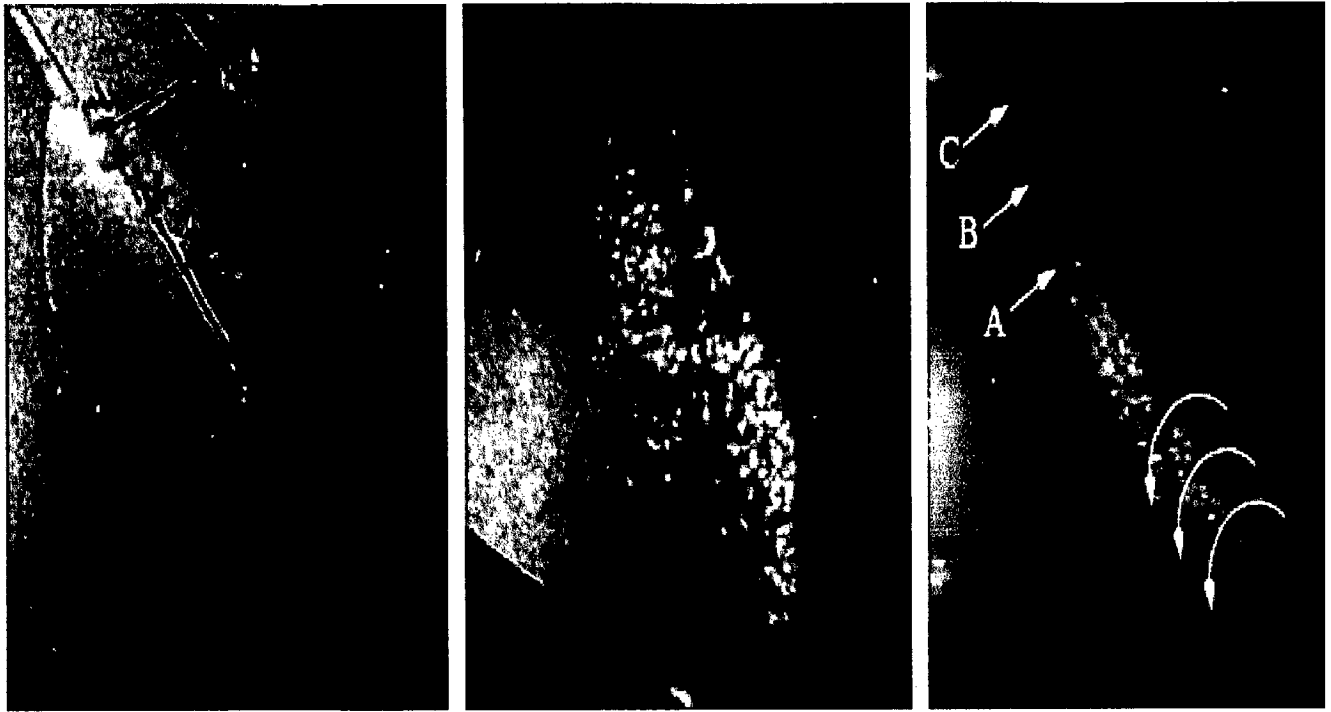
(a)Cavitation initiated close to the fillet between the blade and the flange

(b)More severe cavitation started at the fillet between the blade and the flange

(c)Cavitation at the blade root, with the inner cavity incepted at the fillet and the outer one at the inner corner of the blade leading edge .the direction of the possible weak rotation of the outer cavity can be as shown by the arrows

Fig 3.6 : Cavitation at the blade root

Under conditions of more developed cavitation, as in Figure 3.6(b), the inner root cavity that is initiated at the fillet shows no broken-off structures at the cavity closure. On the other hand, the outer cavity in the figure shows some minor shedding of bubble clouds. When the amount of cavitation at the blade root is increased further by changing the running condition (as in Figure 3.6(c)), the shedding of bubble clouds from the outer cavity appears to increase, whereas the inner cavity still does not show any shed structures. It should be noted that similar root cavitation formations on propellers can exhibit significant shedding of cloud cavitation that results in erosion and noise. The origin of the inner root cavity remains at the fillet even under conditions of more severe cavitation development, as can be seen in Figures 3.6(b) and 3.6(c).

3.5.2.1 Flow disturbance from the inner corner of the blade leading edge (Mechanism b)

The influence of the flow disturbance from the corner, between the blade leading edge and the hub (B in Figure 3.6(c)), on the root cavitation is not obvious under all running conditions. In Figure 3.6(c), it can be seen that the outer cavity originates from the corner between the leading edge of the blade and the hub. When looking for vorticity, it appears that the outer root cavity is not strongly influenced by this either.

3.5.2.2 Flow disturbance from the join between the hub and inner head cover (Mechanism c)

A flow disturbance originating from the join between the rotating hub and the stationary inner head cover (shown at A in Figure 3.6(a)), is observed under conditions of severe cavitation development. which looks like a cavitating vortex which is superposed to the cavities originating from the inner corner of the blade leading edge.

3.5.3 Cavitation at the blade tip

Important mechanisms that influence the cavitation development at the blade tip area are: tip clearance flow, scraping of the boundary layer on the discharge ring wall by the blade tips. It should be noted that a tip vortex, which is caused by tip clearance flow, and a scraping vortex, formed by boundary layer scraping, have opposite rotation directions.

The cavitating tip vortex leaves the blade surface, makes a turn and then approaches the blade surface again. This procedure is repeated a couple of times over the blade length. This pattern is caused by interaction with vortices or wakes, originating from the guide vanes. Wakes that originate from the guide vanes have been reported to appear in Kaplan turbines at the outer cylindrical sections just upstream of the runner, as well as downstream of the runner where they are sliced into pieces. Two mechanisms that conceivably promote vortex generation at the guide vanes are: (1) passage vortices (also called channel vortices) caused by secondary flow, and (2) leakage vortices caused by leakage flow from the pressure side to the suction side of the guide vanes at the lower end of them.

37
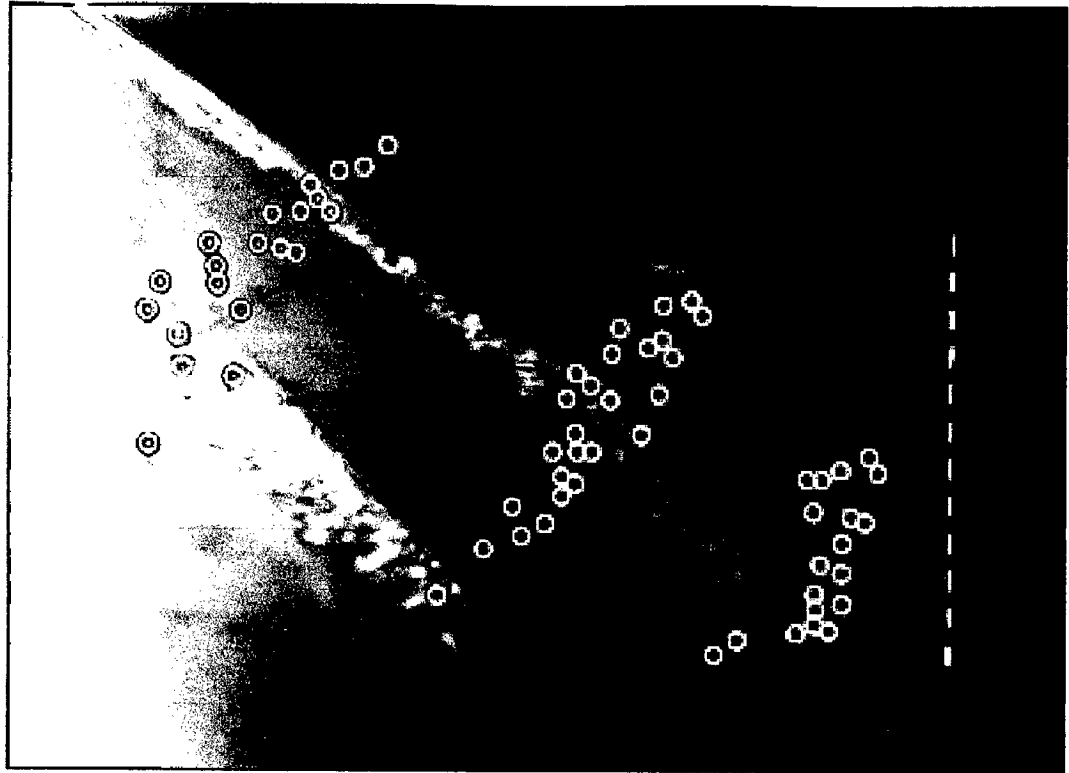
Fig 3.7 Points where the tip vortex makes contact with the blade surface are marked for several blade passages. The contact points appear in bands.

3.6 PARAMETERS AFFECTING INCEPTION AND DEVELOPMENT OF CAVITATION IN HYDROTURBINES

3.6.1 Turbine type and configuration

Cavitation plays an important role in reaction water turbines such as Kaplan, Francis and Pump-Turbine. The main difference between Kaplan and Francis turbines is the design of the runner which is, respectively, axial and radial. For the reversible Pump-Turbine, the runner has a radial design with low specific speed and it can operate in turbine or in pump mode. The rest of the machine components comprising the penstock, spiral casing, stay vanes, guide vanes, draft tube, shaft, alternator and bearings are analogous for any particular design. In Fig 3.8 , a schematic of a Kaplan turbine is shown on the left and a cross section of a Francis runner with its downstream

reservoir is shown on the right. The runner design has a clear influence on the cavitation phenomenon but two other important parameters also influence its inception and development which are the machine setting level and the operation at off-design conditions.

3.6.2 Turbine setting level

The setting level of the machine is the distance Hs indicated in Fig 3.8 that determines the pressure field in relation to the vapour pressure threshold. For instance, bubble cavitation can appear even at the best efficiency point of the machine because it has a strong dependence on this level. Thus, the cavitation coefficient of a hydraulic turbine depends on this parameter. The International Electrotechnical Commission (ICE) recommends using the Thoma number or plant cavitation number σ_p[10] defined as

$$\sigma_p = \frac{NPSE}{E}$$

where E is the specific energy and NPSE is the net positive suction specific energy that in turn can also be calculated as

$$NPSE = \frac{p_i}{\rho} - g(Z_i - Z_{ref}) + \frac{1}{2}C_i^2 - \frac{p_v}{\rho}$$

or

$$NPSE = \frac{p_a}{\rho} - gH_s + \frac{1}{2}C_i^2 - \frac{p_v}{\rho}$$
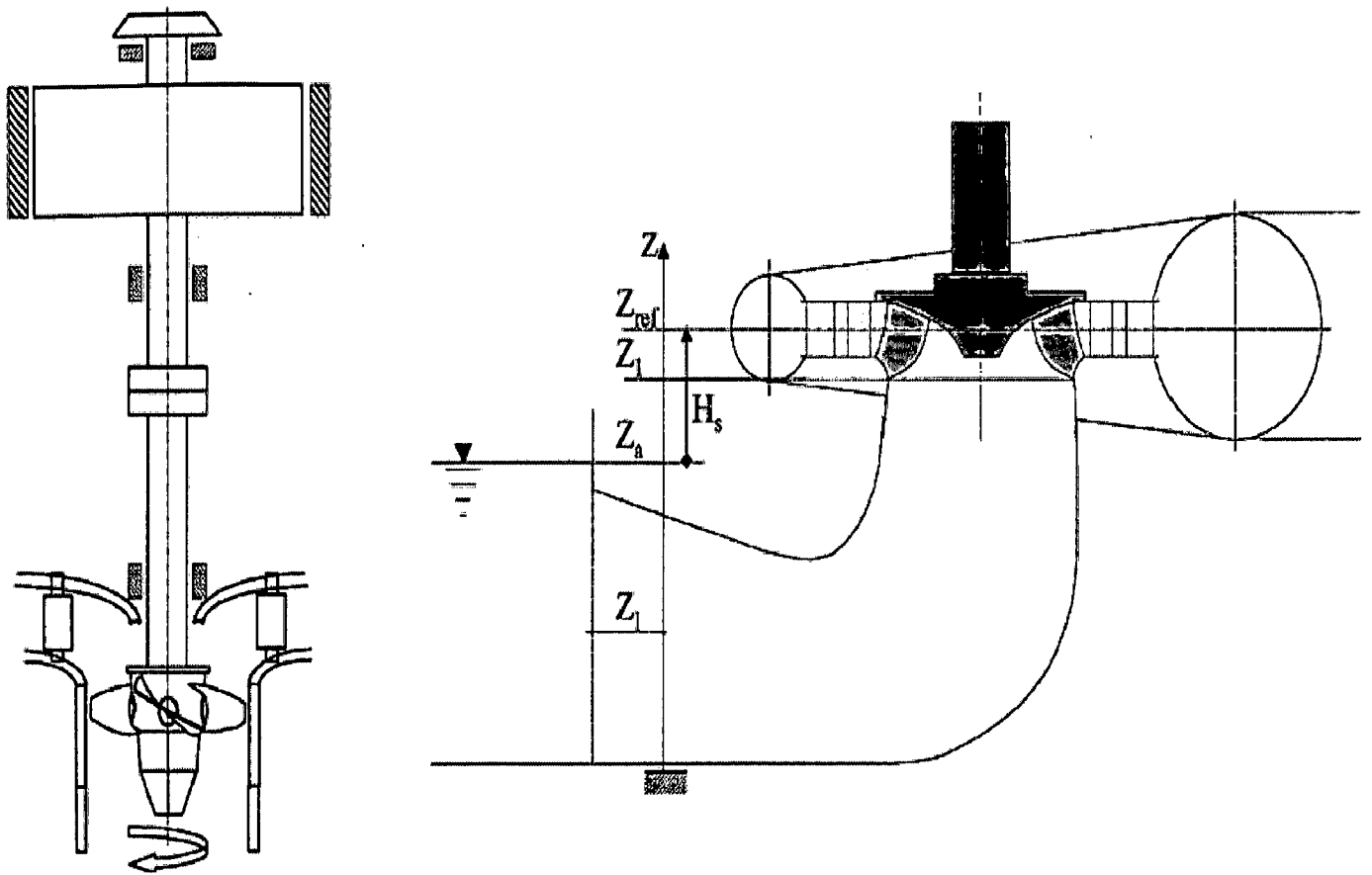
Fig 3.8. (Left) Schematic of a Kaplan turbine and its mechanical configuration. (Right) Schematic of a Francis .

3.6.3 Turbine operation

A water turbine is designed to have the maximum efficiency for a given head and flow rate, but it can also operate at off-design points. As an example, the typical diagram for a Francis turbine is shown on the left of Fig. 3. The operating point is determined by the pressure or head coefficient, ψ; [10] defined as

$$\psi = \frac{2E}{\omega^2 R^2}$$

and by the flow coefficient φ, defined as

$$\varphi = \frac{Q}{\omega \pi R^3}$$

The sub-index $_\Lambda$ denotes the best efficiency or design point. Nevertheless, the head can change because the upstream or downstream reservoir levels may vary. On the other hand, the flow rate is changed by opening or closing the guide vane angle, β; in order to regulate the power output (see the schematic on the right of Fig. 3.9). These variations have a direct influence on the kinematics of the flow trough the runner that in turn determines the tendency to promote cavitations. The absolute fluid velocity in a fixed frame of reference is denoted by C and the relative velocity in a rotating frame of reference is denoted by W (subscripts 1 and 2 designate particular values at runner inlet and outlet). They are related by U which is the tangential velocity. Then, the angle between W and the tangent to the blade at the leading edge is the incidence angle, α; of the incoming flow. If, for instance, there is an increase of head for a given guide vane angle, β; the absolute fluid velocity C_1 will grow and the incidence angle, α; that for the design condition is very small and close to zero, will become positive. Consequently, when the machine operates at higher heads than design ones ($\psi/\psi_\Lambda \gg 1$), attached cavitation can appear in the suction sides of the blades. Obviously, the velocity vectors at the outlet are also modified if the inlet conditions change. For example, the absolute velocity C_2; which has a radial direction at the best efficiency point, can change and leave a residual circumferential component affecting the draft tube flow.
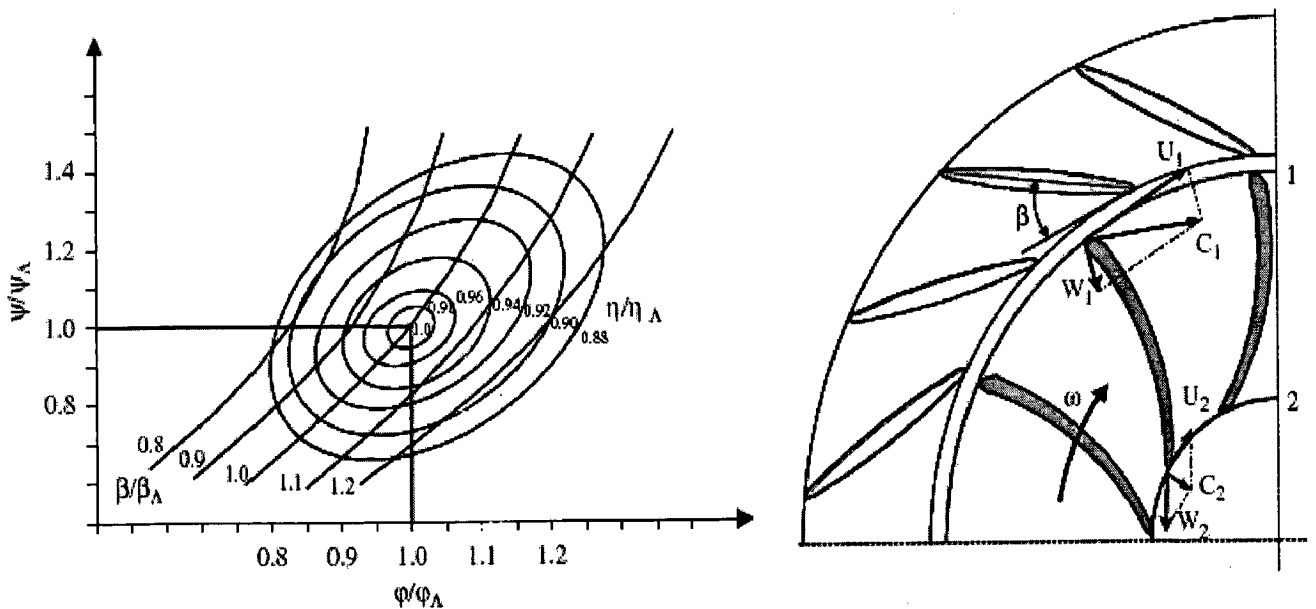
Fig 3.9. (Left) Typical operating range for a Francis turbine. (Right) Vector diagrams describing the kinematics of the flow through a Francis turbine runner.

3.7 BASIS OF DIFFERENT ANALYTICAL MODELS TO DETERMINE CAVITATION EROSION

1. An analytical model for the prediction of cavitation erosion of ductile materials is based upon a physical analysis of the work-hardening process due to the successive bubble collapses. The material is characterized by its classical stress-strain relationship and its metallurgical behaviour is analysed from microhardness measurements on cross sections of eroded samples. The flow aggressiveness is determined from pitting tests, using the material properties to go back to the impact loads.

The first step of the model consists of the quantification of the hydrodynamic aggressiveness of the cavitating flow which can be done from classical pitting tests, each pit being characterized by its diameter and its depth. The surface distribution of the impact load responsible for each pit can be deduced from couple of data, using the strain profile and the stress-strain relationship of the material. The flow aggressiveness can be finally characterized by a distribution of impact loads.

In a second step, the distribution derived from short duration tests is numerically applied a large number of times on the material surface and the mass-loss as a function of the exposure time can be computed[14]

2. An expression for the maximum energy absorbed per unit volume of the plastically deformed layer of the material surface by the help of readily obtainable material properties can be obtained. Secondly the cavitation processes are considered and the energy flux which is able to cause plastic deformation is evaluated except for a constant of proportionality as a function of the cavity density, the cavity size distribution, the cavity distribution normal to the material surface, the hydrostatic pressure and appropriate material properties. Thirdly these calculations are compared and expressions for the cavitation erosion resistance and the incubation period are found for different cavitation systems.[15]

3. In other model deformation rate of the specimen surface by the collapse of a single cavity can be estimated from bubble dynamic considerations.

4. On the basis of turbine submergence or the setting of hydraulic turbine, number of runner blades, the turbine throat velocity and the turbine runner material an empirical relation for

the cavitation erosion can be determined and which can than be used as an important tool for the prediction of cavitation erosion up to certain extent. The gamma concept developed by J.L Gordan is found useful for the same. A set of empirical equations has been developed which defines the peak efficiency and shape of the efficiency curve for hydraulic turbines as a function of the commissioning date for the unit, rated head, rated flow, runner speed, and runner throat or impulse turbine jet diameter. He demonstrated that the setting of a hydraulic turbine is function of the number of runner blades (b) and the turbine throat velocity (v)[16]. By changing the reference level from the top of the runner to the runner shaft in horizontal axis units, it was found that the equation could be used to define submergence for all reaction turbines.

CHAPTER-4

DESCRIPTION OF RELATIONS USED FOR ANALYSIS

4.1 GENERAL

As it has been discussed in previous chapter that important parameters on which inception and development of cavitation in hydro turbines depends is the turbine type and configuration, turbine setting level and turbine operation so considering this a relation or model or mathematical empirical relation should be there to correlate all these parameters with cavitation erosion. An empirical equation for estimating cavitation metal loss could be a valuable tool in assessing a new runner design, to determine the lifetime operating cost. Such relations, which can be satisfactorily used to determine the optimum submergence level so that the cavitation erosion is within permissible limits as well as the cavitation erosion for the runner was developed by J.L.GORDAN. Similarly he introduced gamma concept so as to indicate that turbines, which are set with less submergence than required submergence, would cavitate more than turbines, which were set deeper.

4.2 PREMILINARY EQUATION

The preliminary relationship used to develop equations for the runner setting, which included factors for the type of runner material, no. of runner blades , turbine throat velocity and the acceptable level of cavitation is as follows[21]:

$$S_t = (4.46b^{-0.56} + XC_f) \; V^2 g^{-1} - B + Y \quad .... \quad (1)$$

where

S_t="theoretical" turbine submergence in meter below tail water to: (1) Shaft centerline on horizontal-axis units; (2) runner-blade centerline on vertical-axis propeller units; and

(3) a point 0.257D below the casing centerline on vertical-axis Francis units,

where D = the runner throat diameter. S, is positive below tailwater and negative above, as shown in Fig

V = turbine axial gross throat velocity with no deduction for hub area (m/s)

b = number of runner blades

g = acceleration caused by gravity =9.81 m/s^2

B = barometric pressure less water vapour pressure at tailwater level (in meters of water pressure) determined from

$$B = 10.3 - 0.002E^{0.92} - 0.01T. \ \dots\dots\dots\dots\dots\dots(2)$$

where:

E = tailwater elevation (m)

T = water temperature (^{0}C)

where X and Y are factors which are a function of the type of runner material and the acceptable cavitation level, and

have values as shown in Table below

Table 4.1 Values of X and Y factors a function of the type of runner material

Condition	X	Y
Carbon Steel runner	0.3	-2.3
Stainless Steel runner	0.2	-2.4

4.3   GAMMA CONCEPT

It can be reasoned that with the empirical equation for turbine setting, turbines that were set higher than S_t, should exhibit more cavitation than those set lower than S_t. To measure this difference, the concept of gamma (γ) was introduced:

$$\gamma = S_a - S_t + 10 \ \dots\dots\dots\dots\dots\dots(3)$$

where Sa = the actual submergence.

Since cavitation commences when the pressure drops below atmospheric pressure (10.33-m water head), and to avoid negative numbers so that data can be plotted on log-log paper, 10 was added to the difference between actual and empirical submergence. In effect, gamma is an approximate measure of the absolute pressure at the runner under full-load flow conditions[20].
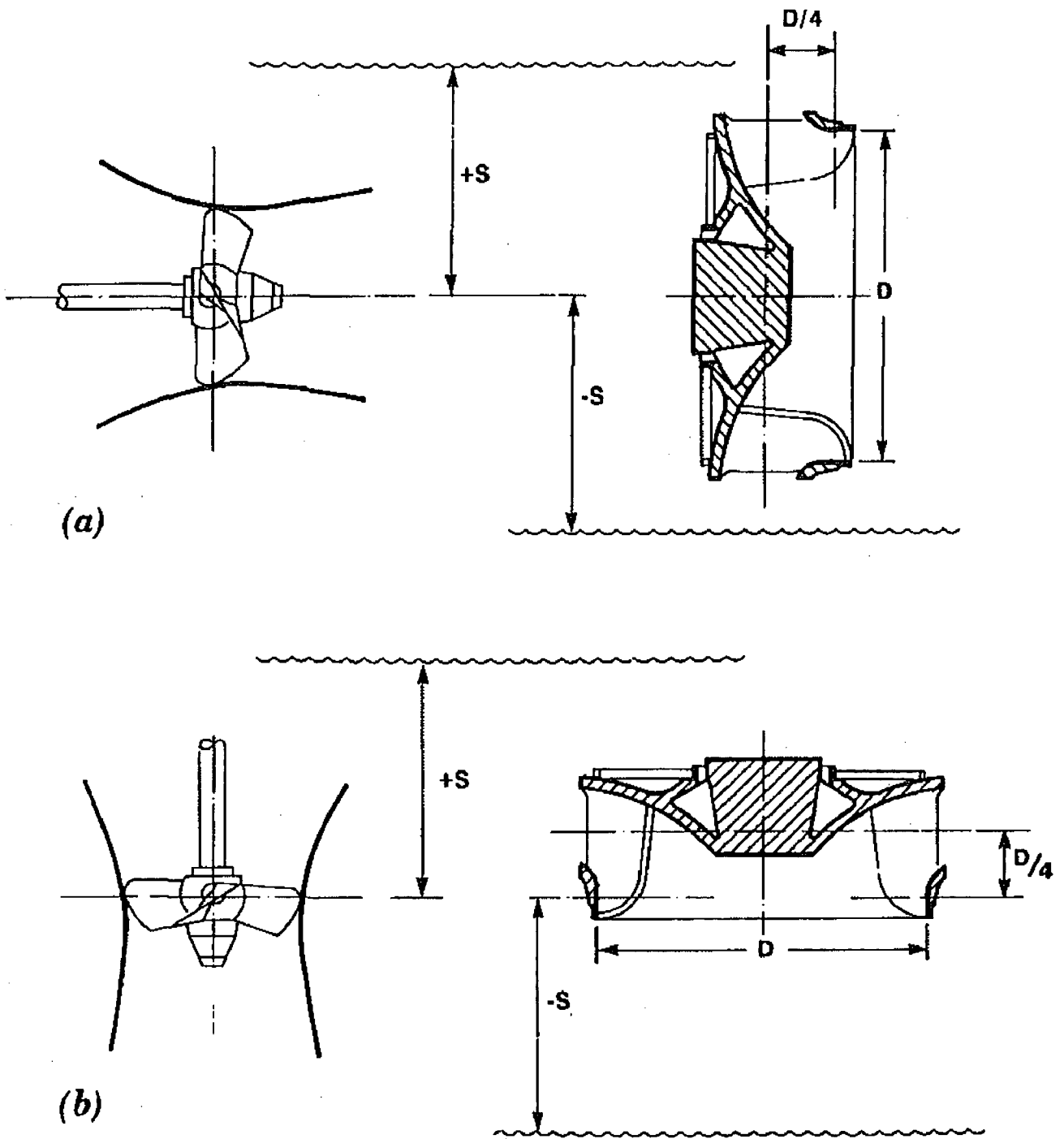
FIG 4. 1. Method Used to Measure Turbine Submergence: (a) Horizontal-Shaft Submergence Measurement; and (b) Vertical-Shaft Submergence Measurement[20]

4.4 EXPANDED SUBMERGENCE EQUATION

Expanded submergence equation was used in an extensive analysis of cavitation records for 208 turbines in the USA obtained from an EPRI report . The work produced a more detailed equation for turbine setting , which included terms for plant capacity factor and runner material:

$$S_t = 0.45V^2b^{-0.56} + 2.3C_f - B - R \dots\dots\dots\dots\dots\dots(4)$$

where R is a runner material factor with a value of:

R = 1.2 for a carbon steel runner

= 1.7 for a bronze runner

= 2.9 for a stainless steel runner

= 2.2 for a: carbon steel runner with stainless overlay.

However Cavitation erosion in a turbine is difficult to measure with precision methods range from using the weight of the weld rod required in a repair the volume of a putty or other substance used to fill the cavitation holes. To bring all turbines to a common base, the weight of reported metal lost in kilograms is divided by the runner diameter squared, and by the number of operating hours since the last repair. This number is then multiplied by 8000 (hours per annum) to obtain a cavitation factor k. Since gamma ranged over less than one magnitude, from about 5 to 17, and cavitation intensity ranged over at least four magnitudes, from 0.001 to 10, the data were plotted on semilog paper as shown on Fig 4.2 above and it became evident that the relationship between gamma and cavitation intensity could be expressed by

$$\gamma = 8.4 - log_n k_1 \qquad \dots\dots\dots\dots\dots\dots\dots\dots(5)$$

where k_1 = the runner suction-side metal loss in 8,000 hours of operation, divided by the square of the runner throat diameter ie.

$$k_1 = 8000Wd^{-2} \dots\dots\dots\dots\dots\dots\dots\dots(6)$$

= turbine runner cavitation index

W = metal loss from suction side of turbine runner blades (in kg/h)

d = turbine runner throat diameter (m)

Above equations Eqs. (3), (4), and (5) can now be combined to eliminate gamma and S_t producing a relationship between setting and cavitation erosion[20]:

$$S = 0.45V^2 b^{-0.56} + 2.3C_f - B - R_1 - \log_n k_1 \dots\dots\dots\dots\dots\dots(7)$$

where the value of R_1 is given by:

R_1 = 2.8 for carbon steel runners

    = 3.3 for bronze runners

    = 4.5 for stainless steel runners

    = 3.8 for carbon runners with stainless steel overlay

Table below provides suggested values for $\log_n k_1$ based on a review of fig 4.2 above, where there is a difference of just over 5 m in the range of settings; the lower setting, - 5.85 m, corresponds to a 95% confidence of attaining minimal cavitation, and the upper setting, -0.87, to a 75% confidence of not exceeding the upper cavitation limit according to the International Electro-technical Commission, Geneva, Switzerland (IEC), of $k_1 = 1.9$

TABLE 4.2 : Suggested Values of $\log_n k_1$, to be Used in Eq. (7) to Establish Turbine Setting[20]

Acceptable degree of cavitation	k_1	Desired confidence and Required value of $\log_n k_1$	
		75 %	95 %
None to minimal	0.025	-5.15	-5.85
Lower IEC limit	0.47	-2.21	-2.91
Upper IEC limit	1.90	-0.87	-1.57
Note: IEC = International Electrotechnical Commission			
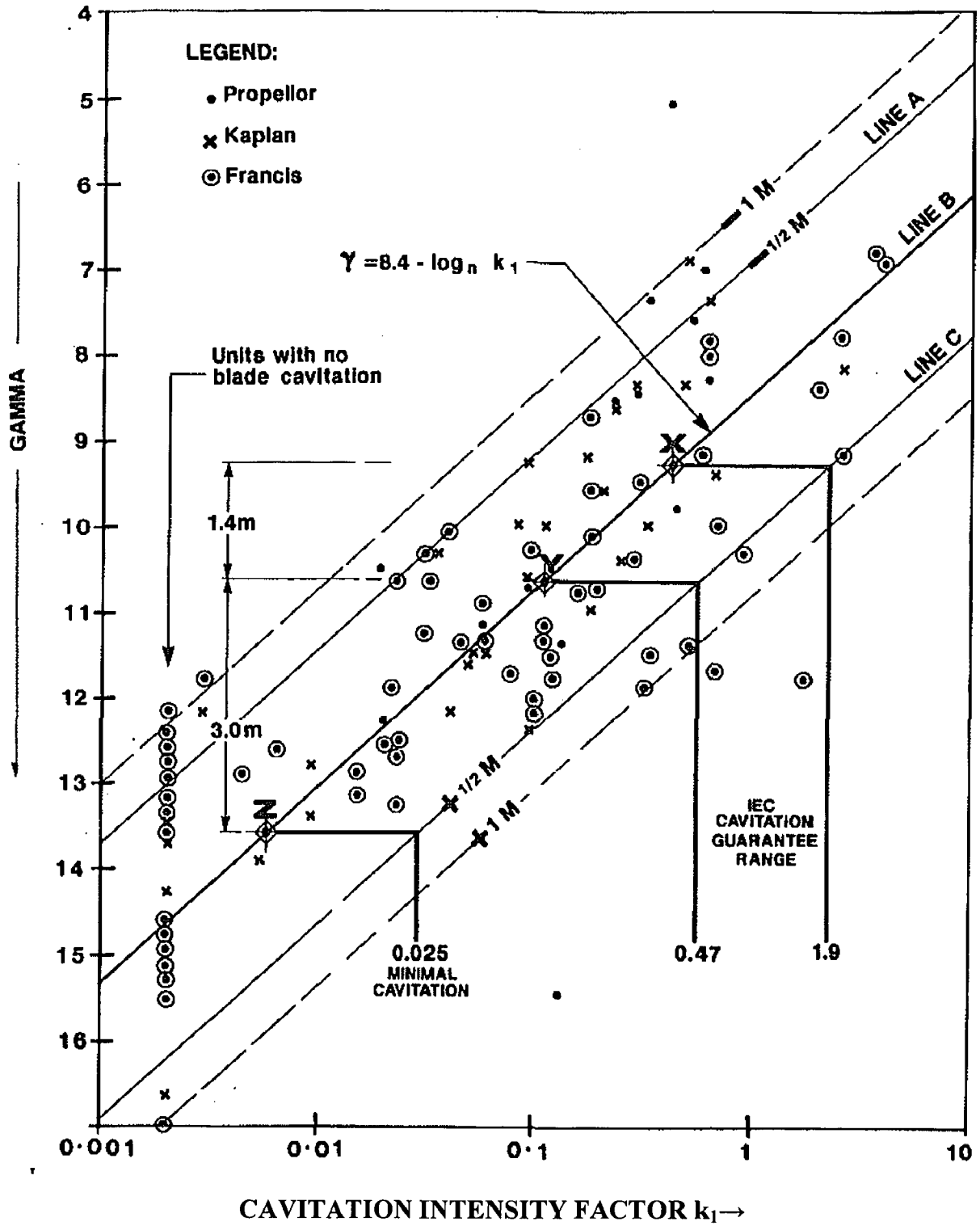
FIG. 4.2. Relationship between Gamma and Cavitation Intensity Factor k_1, using Data from EPRI Survey plus (3) and (4) to Derive Value of Gamma[16],[20]

4.5   CAVITATION EROSION EQUATION

The expanded submergence equation can be rewritten with turbine runner cavitation index equation to obtain the expression for the weight of metal lost during a time period of 8000h as[16]:

$$W = d^2 \, 2.718^{\,m} \quad\text{.............................(8)}$$

where m =cavitation exponent, calculated by:

$$m = 0.45V^2 b^{-0.56} + 2.3C_f - B - R_1 - S_a \quad\text{.........................(9)}$$

To ensure that the full range of cavitation experience is covered equation for cavitation erosion can be restated as[16]:

$$W_t = k_2 d^2 \, 2.718^{\,m} \quad\text{.........................(10)}$$
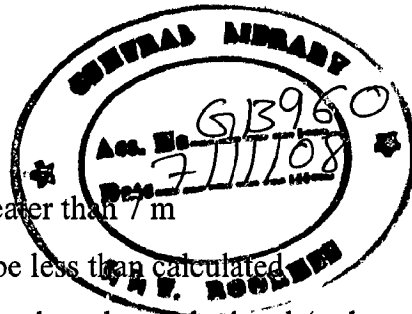
where: k_2 =1(median value) to be used for runner throat dia greater than 7 m

=5, to be 75 per cent certain that the cavitation will be less than calculated

= 10, to be 95 per cent certain that cavitation will be less than calculated (to be used for cast runners with runner diameter less than 2 m)

The final above equation can now be used to determine probable extent of cavitation in a new turbine runner, and it can be used to determine the cavitation potential of different designs.

4.6   LOSS OF EFFICIENCY WITH MASS LOSS

Due to mass loss of the turbine efficiciency of the turbine deteriorates and thus efficiency can be expressed as a function of mass loss as follows.[21]

$$Eff_{wl} = K \times M^{-a} \quad\text{.............................(11)}$$

Where ,

Eff_{wl} = predicted efficiency with mass loss

M = Mass loss

a = 0.00500250124054351

K = 0.717840050298804 (for pelton and high head schemes)

50

So it can be seen from the relation that mass loss is inversely proportional with a power raised to the efficiency .But it cannot be used as such for our purpose since value of K is applicable to pelton and high head schemes but assuming that the equation will give equally good results when applied to Chilla by giving the constant a K value of 0.92 (the full load turbine efficiency).So now the new efficiency due to mass loss will now deprecate corresponding to the full load designed efficiency of the turbine at Chilla project.

CHAPTER-5

ANALYSIS OF EROSION DUE TO CAVITATION OF CHILLA AND DHUKWAN - CASE STUDIES

5.1 GENERAL

As discussed earlier the quantum of erosion due to cavitation can be assessed by knowing the setting or the submergence of the hydro turbine and the theoretical or optimum submergence can be determined by the analysis done in previous chapter and now based on this the analytical study will be carried out for an existing actual site i.e. Chilla Hydro Power Project, Rishikesh and than theoretical submergence can be given for a raw site Dhukwan in Jhansi.

5.2 SALIENT FEATURES OF GHARWAL – RISHIKESH - CHILLA HYDEL SCHEME

Garhwal Rishikesh Chilla Scheme is one of the run of the river schemes located in UTTARANCHAL state and is owned by Uttaranchal Jal Vidyut Nigam Limited . It utilizes a drop of 33 metres from Virbhadra upto power house situated 4 km. upstream of Ganga Canal Headwork's at Bhimgoda. The river discharge available at Virbhadra, has been diverted by constructing a barrage in to a 14.1 km., long power channel. After generating power the water is discharge in river Ganga a 1.2 km long tailrace channel. Works on this scheme were started in Oct. 1974 and all the functional works were completed by Dec. 1980. All the four units of the power house were commissioned in March, 1981. The discharge as available in river Ganga, upto 580 cumecs (20,000 cusecs) has been utilized for generation of power. The total cost of the scheme is 9776 lacs and it has added 742 million units annually. This generation would increase to 920 million units after completion of Tehri Project.

5.2.1 Barrage and Head Regulator at Virbhadra

312 metres long barrage having 15 bays of 18 metres each and 63 metres long head regulator having 5 bays of 11 m each have been constructed on river Ganga at Virbhadra, 5 km., downstream of Rishikesh. This barrage is in boulder stage of river and has been designed for discharge intensity of 67 cumecs per metre.

5.2.2   Power Channel

The power channel, 14.1 km., long runs between left bank of river Ganga and foot hill i exceedingly difficult and torturous terrain with varying geology. At some places it has bee constructed in 30 metres deep excavation and at some places in 30 metres high embankment.

5.2.3   Powerhouse at Chilla

The powerhouse is a surface powerhouse and has four units of 36 MW each utilizing drop of 3 meters. Water is fed in to the turbines through four penstocks of 6 meters diameter each of about 5 meters length. The water from the power house is discharged back in river Ganga, upstream c Ganga Canal head works, through a 1.2 km., tail race channel.

Fig 5.1 Satellite image of Chilla Hydro Power Project
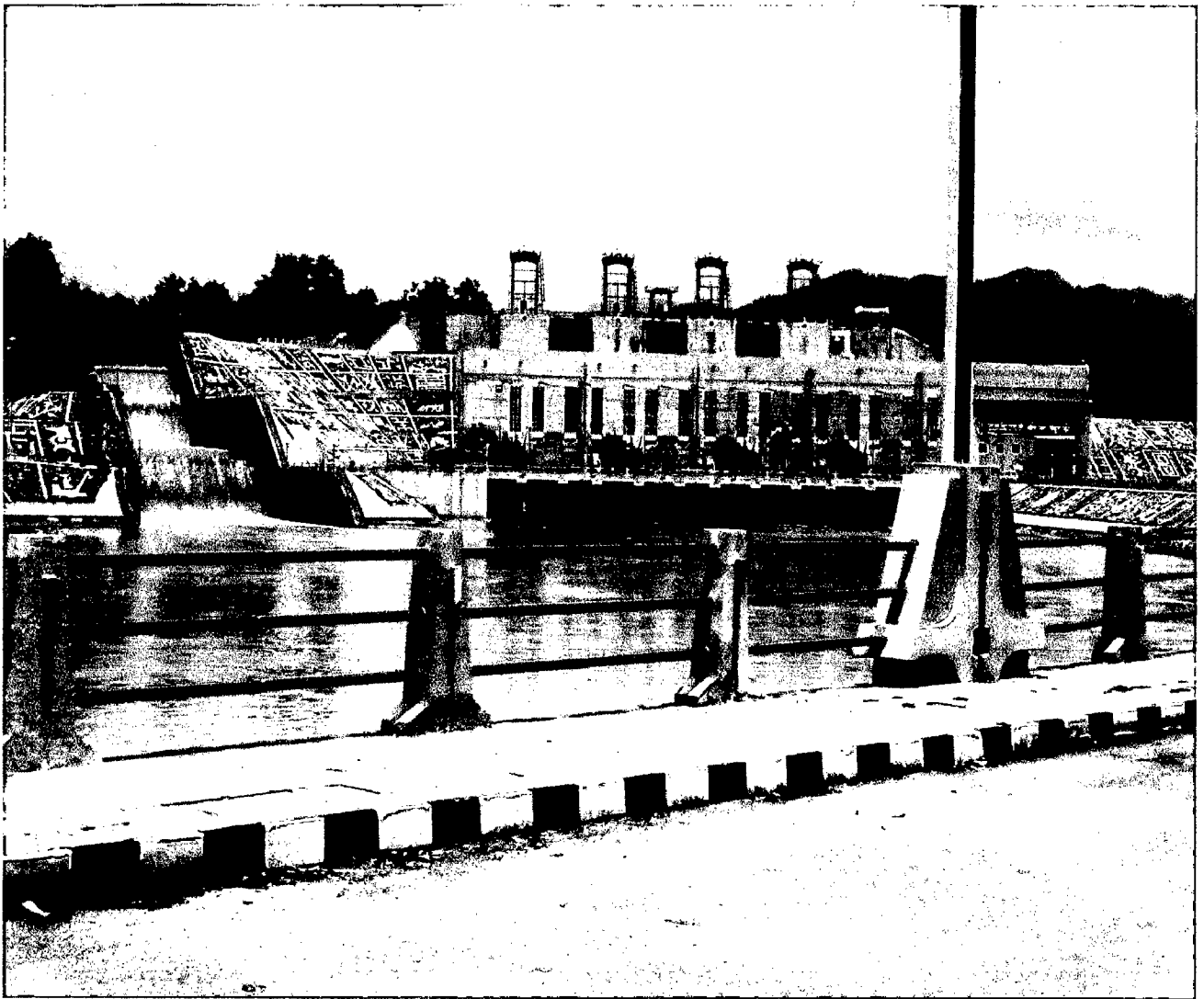
Fig 5.2 Actual Photograph of Chilla Hydro Power Project from tail water side

5.2.4 Salient Features

1. (a) Location of Barrage   Virbhadra

    (b) Location of Power House   Chilla

                                             4 kms upstream of Bhimgoda headworl

2. Hydrology (at Barrage)

    (a) Catchment area   21400 sq km

    (b) 90% available discharge   182.7 cumecs

    (c) design flood   14600 cumecs.

3. Barrage

	(i)	Overall Length	312 m
	(b)	Number of bays	15 bays of 18 m each
	(c)	Number and size of	
		(i) under sluice gates	4 nos. 8 x 18 m (bottom tier)
			4 nos. 3.15 x 18 m (top tier)
		(ii) weir bays gates	11 nos. 10.15 x 18 m
	(d)	Pondage Capacity	4.7 M cum (Live-storage)

4. Head Regulator

	(a)	Overall length	63m
	(b)	Number of bays	5 bays of 11m each
	(c)	Size of gates	7.7 x 11 metre

5. Silt Ejector

	(a)	Width at entrance	42.0 m
	(b)	Opening at entrance	1.6 m high
	(c)	Number of funnels	3 (Each having 4 sub funnels)
	(d)	Discharge	115 cumecs

6. Power Channel

	(a)	Capacity upto 0.2 km from head	680 cumecs
	(b)	Capacity from 0.2 km onward	565 cumecs
	(c)	Total length	14.3 km
	(d)	Bed width	12.5 m
	(e)	Side slopes	1.75:1
	(f)	Bed slope	1 in 6000

7. Forebay & Intake/Penstocks

	(a)	Length of forebay	245 m
	(b)	Bed width	70.70 m
	(c)	Intake Gates	4 nos. 6m x 7.2m
	(d)	Penstocks	4 nos. of 6m dia each

8. Power House

	(a)	Location	At 14.3 km of Power Channel

		(b)	Head	32.5 m

(b)   Head   32.5 m

(c)   Installed Capacity   144 MW(4 Machines of 36 MW)

(d)   Type of machine   Kaplan Type, vertical shaft hydraulic turbine

(e)   Dia of Runner   4.0 m

(f)   Speed   187.5 r.p.m

9.   Tail race channel

(a)   Capacity   565 cumecs

(b)   Length   1.2 Km

(c)   Bed width   75 m

(d)   Bed Slope   1 in 5000

(e)   Side slope   1.75:1

10.   Bypass

(a)   Capacity   565 cumecs

(b)   Water-Way   59.9 m (gross)

(c)   3 falls   7.0, 13.3 &12.7 meter

11.   Generating Plant and Machinery

(a)   Turbine

       (i)   Make   BHEL,INDIA

       (ii)   Nos. & Type   4-V Kaplan

       (iii)   Rated output kW   38300

       (iv)   Net Head   32.5 m

       (v)   Efficiency at full load   92%

       (vi)   Rated Speed   187.5 r.p.m

       (vii)   Runaway speed   385/485 on cam/off cam

(b)   Generator

       (i)   Make   BHEL INDIA

       (ii)   Nos. & Type   4-V Suspension

       (iii)   Rated Output   36 MW
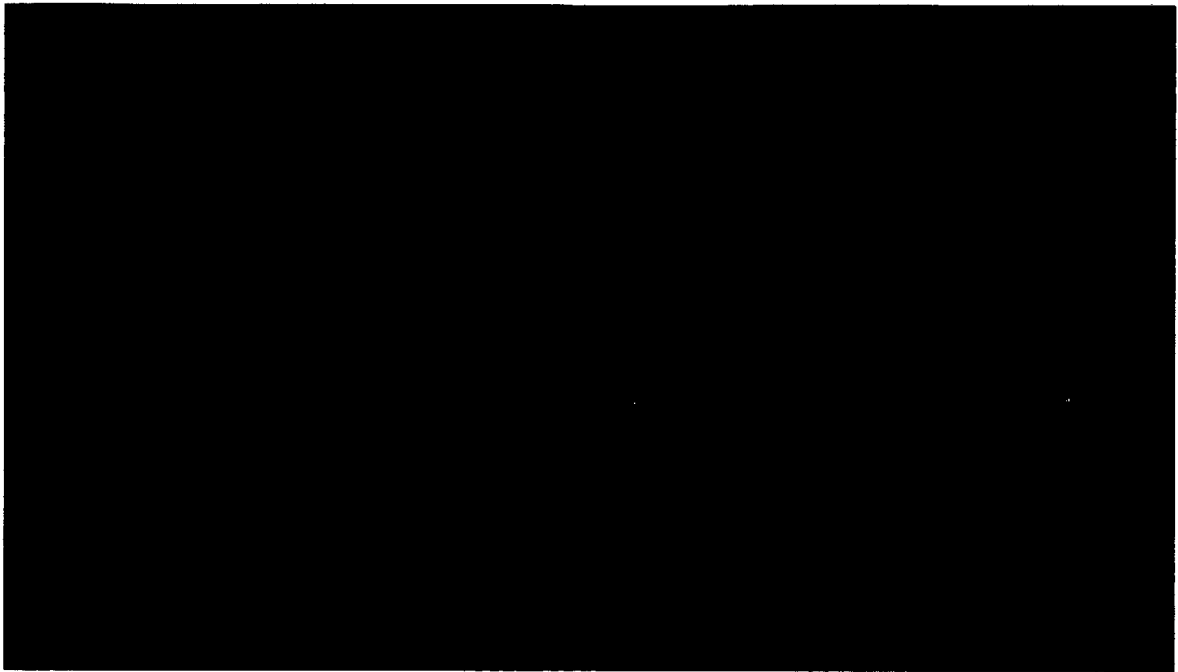
Fig 5.3 Actual annual energy generation of Chilla

5.3 ANALYSIS FOR DETERMINING OPTIMAL TURBINE SUBMERGENCE FOR THE CHILLA HYDRO ELECTRIC PROJECT

For determining the optimal turbine submergence so that the cavitation should be in the International Technical Council, Geneva cavitation guarantee range the three values of k_1 as in table 4.2 can be used and can be proceeded as follows .

5.3.1 Calculations to determine turbine setting for the Chilla Project

Using the equation (7) to determine the submergence

i.e relationship between turbine setting and cavitation erosion:

$$S = 0.45V^2b^{-0.56} + 2.3C_f - B - R_l - log_nk_l \quad \ldots\ldots\ldots\ldots\ldots\ldots\ldots(7)$$

Now Using equation (2) from chapter 4 to determine B

ie. $B = 10.3 - 0.002E^{0.92} - 0.01T \ldots\ldots\ldots\ldots\ldots\ldots\ldots\ldots\ldots(2)$

taking E = Tail water elevation = 296 m ....(From the Chilla control Log book) and $T = 20^0C$

$$B = 10.3 - 0.002x \, 296^{0.92} - 0.01 \times 20$$

	(iv)	Power Factor	0.9 lag
	(v)	Efficiency at full load	97.42%
	(vi)	Voltage	11 KV
	(vii)	Current	2100 A

12. Transmission Lines

(a)	Outgoing feeders	3
(b)	Voltage	132 KV

13. Miscellaneous Features

(a)	Planned Load Factor	57
(b)	Planned energy generation	725 MU
(c)	Costs and Benefits	
	Cost of Project	98 Crores
	1. Civil works	75 Crores
	2. Hydel works	23 Crores

5.2.5 Annual energy generation for Chilla Hydroelectric Project was collected from the power station for the last eight years and is shown in table 5.1 and fig 5.3.

Table 5.1 Actual energy generation at Chilla

Year	Annual generation (real) in MU
2001-2002	560.752
2002-2003	607.398
2003-2004	688.901
2004-2005	746.072
2005-2006	659.181
2006-2007	740.464
2007-2008	826.021

$$B = 10.3 - 0.3755 - 0.2$$

$$B = 9.7245 \text{ m} \dots\dots\dots\dots\dots\dots\dots\dots\dots\dots\dots\dots(11)$$

Now velocity at turbine runner throat can be calculated using the power equation which is as follows:

$$O = 9.81 \times 0.785 d^2 \, Vhe \dots\dots\dots\dots\dots(12)$$

where O = the turbine full-load output at rated net head (kilowatts)

Substituting the values as

Runner Diameter (d) = 4m.............................(From turbine data)

Net Rated head of the turbine (as per turbine specification) = 32.5 m

Efficiency at full load (e) = 92%

Turbine full load output = 38300 Kw.................(From turbine data)

So substituting all required values in (12)

$$V = \frac{O}{9.81 \times 0.785 \times d^2 he}$$

$$V = \frac{38300 \ (Kw)}{9.81 \times 0.785 \times 4^2 \times 32.5 \times 0.92}$$

$$V = 10.39 \text{ m/s} \sim 10.4 \text{ m/s}\dots\dots\dots\dots\dots(13)$$

Now substituting the Value of B and V from (11) and (13) respectively in Equation (7) and

No. of runner blades(b) = 6   (from turbine data)

Value of R for stainless steel runners overlay = 3.8

And the plant usage factor C_f = 0.57 ....(From data collected)

i.e. $S = 0.45V^2 b^{-0.56} + 2.3C_f - B - R_l - log_n k_l$

Case 1.   For cavitation to be none to minimal according to figure 4.2 and table 4.2 k_1 = .025

$$S = (0.45 \times 10.4^2 \times 6^{-0.56}) + (2.3 \times 0.57) - 9.7245 - 3.8 - \ln 0.025$$

59

$$S = 9.32038 \text{ m} \dots\dots\dots\dots\dots\dots(14)$$

Case 2.   Similarly for cavitation to be at the lower limit of the IEC Cavitation guarantee range and taking $k_1 = 0.47$ from fig 4.2 and table 4.2

$$S = (0.45*10.4^2 * 6^{-0.56}) + (2.3*0.57) - 9.7245 - 3.8 - \ln 0.47$$

$$S = 6.3864 \text{ m} \dots\dots\dots\dots\dots\dots\dots(15)$$

Case 3.   Again For determining the upper limit of the IEC cavitation guarantee range by taking $k_1 = 1.9$ from fig 4.2 and table 4.2

$$S = (0.45*10.4^2 * 6^{-0.56}) + (2.3*0.57) - 9.7245 - 3.8 - \ln 1.9$$

$$S = 4.9895 \dots\dots\dots\dots\dots\dots\dots\dots(16)$$

So from this analysis it can be said that submergence for the Chilla site under analysis should be somewhere between 6.38642 m to 9.32038 m .

To have greater in depth analysis so as to obtain a final and concluding picture of the submergence the calculation of the loss of weight in hydro turbine in kg/hour in these three cases is must which can be done by using equation (6) from chapter 4

i.e $$k_1 = 8000 W d^{-2}$$

and for getting mass loss in 8000 hours we can use

$$W = k_1 x d^2$$

So

Case 1.   For cavitation to be none to minimal according to figure 4.2 and table 4.2 using $k_1 = .025$

$$W = (.025 \text{ x } 16) \text{ Kg}$$
$$W = 0.4 \text{ Kg}$$

Case 2.   Similarly for cavitation to be at the lower limit of the IEC Cavitation guarantee range and taking $k_1 = 0.47$ from fig 4.2 and table 4.2

$$W = (0.47 \text{ x } 16) \text{ Kg}$$

$$W = 7.52 \text{ Kg}$$

Case 3.   Again For determining the upper limit of the IEC cavitation guarantee range b

taking k_1=1.9 from fig 4.2 and table 4.2

$$W = (1.9 \times 16) \text{ Kg}$$

$$W = 30.4 \text{ Kg}$$

Using the calculated weight loss and corresponding submergence following graph gives a better ide
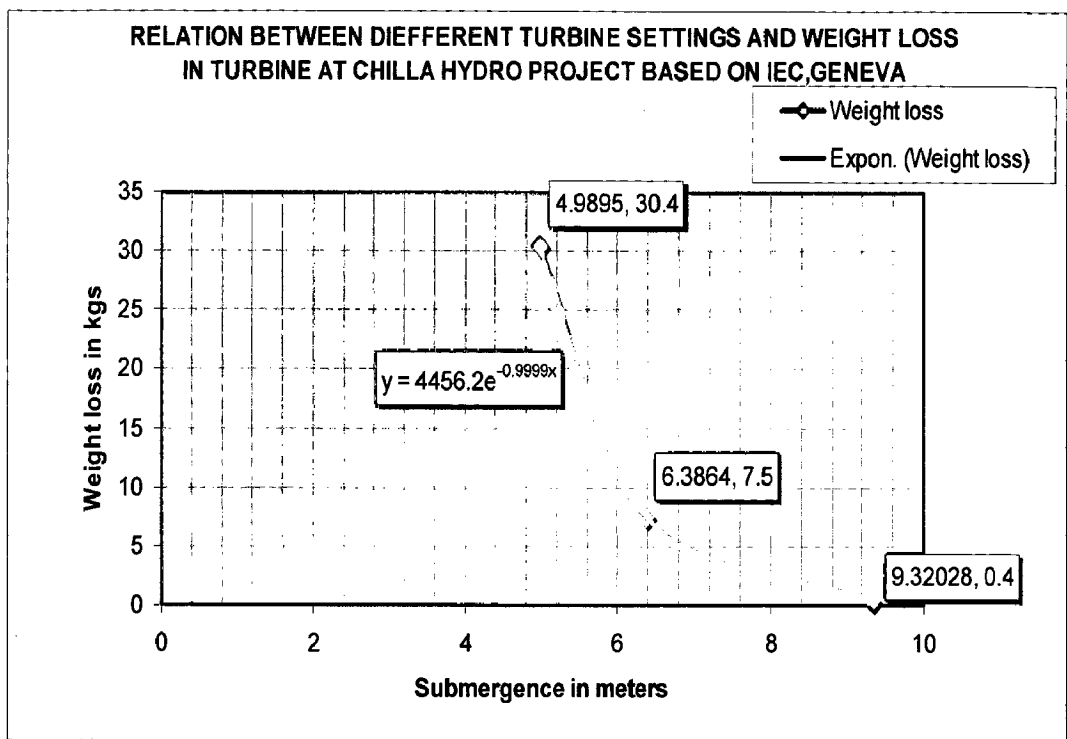
Fig 5.4 Variation of weight loss with increasing submergence

Thus the above curve shows the entire range for the setting of the hydro turbine according to IE

Geneva for the Chilla Hydro Electric Project . Similarly all the three case can be presented in th

histogram as shown

RELATION BETWEEN SUSUBMERGENCE ,LOSS OF WEIGHT AND CAVITATION INTENSITY FACTOR FOR CHILLA

	1	2	3
Submergence	4.9895	6.3864	9.32028
Mass loss	30.4	7.52	0.4

1.9	0.47	0.025

Cavitation Intensity Factor k

Fig 5.5 Relation between submergence,weight loss and cavitation intensity factor for Chilla

Taking the ongoing analysis further and giving the confidence limits to the analysi according to the table 4.2 and fig4.2 we can give the confidence limits of 75% and 95% and tha applying them to each case we have discussed earlier we can determine the new submergence b using the equation (7) from chapter 4

i.e $\quad S = 0.45V^2b^{-0.56} + 2.3C_f - B - R_1 - log_nk_1$

The values of log_nk_1 can be directly used from table 4.2

Case 1.(a) For cavitation to be none to minimal and to be 75% certain that cavitation erosion will be less than calculated, the value of $log_nk_1 = - 5.15$ can be directly taken from the table 4.2 to determine the submergence by substituting it the equation (7)

$$S = (0.45*10.4^2* 6^{-0.56}) + (2.3*0.57) - 9.7245 - 3.8 - (-5.15)$$
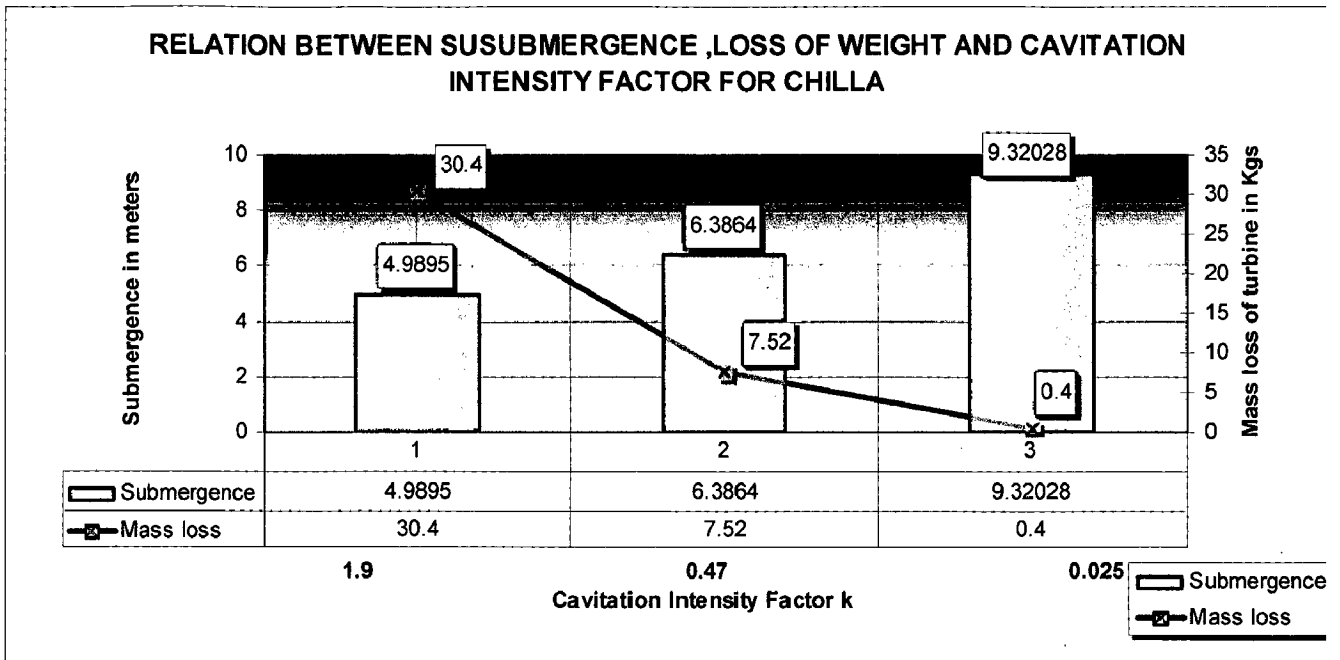
$$S = 10.7815 \text{ m}$$

(b) For cavitation to be none to minimal and to be 95% certain that cavitation erosion will be less than calculated, the value of $log_nk_1 = 5.95$ can be directly taken from the table 4.2 to determine the submergence by substituting it the equation (7)

$$S = (0.45*10.4^2* 6^{-0.56}) + (2.3*0.57) - 9.7245 - 3.8 - (-5.95)$$

$$S = 11.5815 \text{ m}$$

Case 2.(a) For cavitation to be at the lower limit of the IEC cavitation guarantee range and to be 75% sure that cavitation erosion will be less than calculated, the submergence can be calculated using value of $log_n k_1 = -2.21$ from table 4.2 in equation (7)

$$S = (0.45*10.4^2* \ 6^{-0.56}) + (2.3*0.57) - 9.7245 - 3.8 - (-2.21)$$
$$S = 7.8415 \text{ m}$$

(b) For cavitation to be at the lower limit of the IEC cavitation guarantee range and to be 95% certain that cavitation erosion will be less than calculated, the submergence can be calculated using value of $log_n k_1 = -2.91$ from table 4.2 in equation (7)

$$S = (0.45*10.4^2* \ 6^{-0.56}) + (2.3*0.57) - 9.7245 - 3.8 - (-2.91)$$
$$S = 8.5415 \text{ m}$$

Case 3.(a) For cavitation to be at the upper limit of the IEC cavitation guarantee range and to be 75% sure that cavitation erosion will be less than calculated, the submergence can be calculated using value of $log_n k_1 = -.87$ from table 4.2 in equation (7)

$$S = (0.45*10.4^2* \ 6^{-0.56}) + (2.3*0.57) - 9.7245 - 3.8 - (-.87)$$
$$S = 6.501 \text{ m}$$

(b) Again For cavitation to be at the upper limit of the IEC cavitation guarantee range and to be 95% certain that cavitation erosion will be less than calculated, the submergence can be calculated using value of $log_n k_1 = -1.57$ from table 4.2 in equation (7)

$$S = (0.45*10.4^2* \ 6^{-0.56}) + (2.3*0.57) - 9.7245 - 3.8 - (-1.57)$$
$$S = 7.201 \text{ m}$$

All the above analysis can be shown in tabulated form as follows

Table 5.2 Submergence in three cases according to IEC , Ge

Confidence Weights in percentage	Submergence in (m) for cavitation to be none to minimal (CASE 1)	Submergence in (m) for cavitation to be at the lower limit of IEC cavitation gurantee range (CASE 2)	Submergence in (m) for cavitation to be at the upper limit of IEC cavitation gurantee range (CASE 3)
75%	10.7815	7.8415	6.501
95%	11.5815	8.5415	7.201

And the above table can shown in the graphical form as below

FIGURE SHOWING SUBMERGENCE IN (m) FOR 75% AND 95% CONFIDENCE WEIGHTS
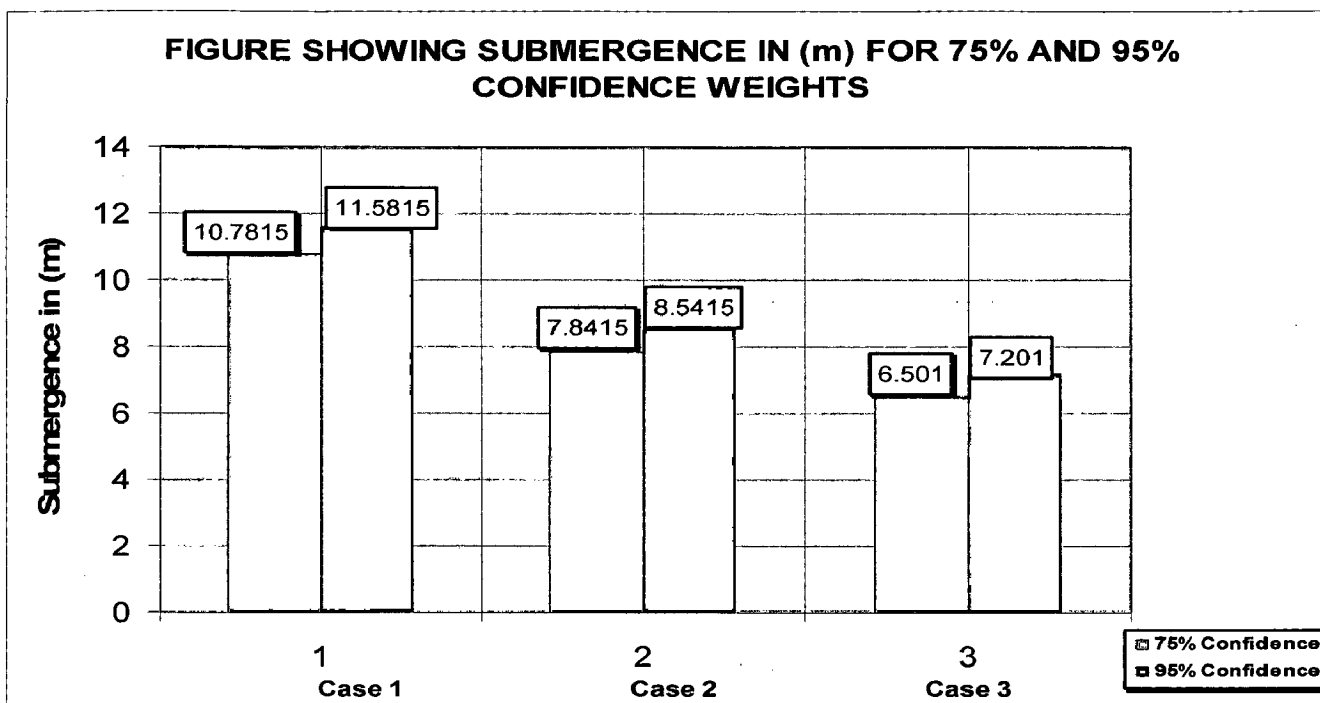
Fig 5.6 Comparing Submergence of 75% and 95% confidence weights

Thus we have determined different submergence limits with the help of the fig 4.2 and table 4. according to the IEC cavitation guarantee range , So before moving ahead in the discussion we sha now determine the actual submergence at the site .

Actual submergence at the site can be determined by determining the elevation levels of th Tail race and turbine runner center line and than deducting the runner centerline elevation from ta water level which is evident and as shown in fig 4.1 . The respective elevation levels can b determined from drawing showing the transverse section through the centerline of the unit . A evident from the drawing the respective elevations from mean sea level are

TWL = 296.00 m (From Chilla control log book)

Runner Centerline = 289.016 m (as confirmed from drawing no. 52300005 in Chilla)

So the actual submergence = TWL - Runner Centerline Level

Actual Submergence = 296.00 m - 289.016 m

$Submergence_a = 6.984$ m ....(17)

Now as we have determined the actual submergence at the Chilla Hydro Power Project our aim now to determine the theoretical optimum submergence using equation (4) in chapter 4 and with th final analysis done in this chapter so as to reach at a concluding value and than to determine th

extra weight loss than the weight loss due to actual submergence at sight and finally to calculate the loss in efficiency due to excessive mass loss which directly effects the annual generation of the plant and can thus result in loss of revenue .

However before using equation (4) to determine optimum submergence some judgment is needed as it is most accurate for run-of-river plants where there is little variation in tail water level. This accuracy could be improved by obtaining hourly data on turbine flow and tail water levels, and integrating the data over one year, to obtain a better value for the relationship between submergence and cavitation. Data from Fig. 4.2 can be used to select an appropriate turbine setting , based on the acceptable level of cavitation erosion and the desired risk of being within the erosion rate. For instance, it would be prudent to accept only minimal cavitation in a small Francis-type runner, where access into the runner for cavitation repair is not possible due to the restrictive small water passages. On the other hand, some cavitation could be accepted on a larger runner operated to provide peak load power, where both access and time are available to permit repairs.

Chilla Hydro Power Project is a run off river scheme and therefore tail water variation is very little and moreover the maintenance schedule is yearly and the runner is large where both access and time is easily available so based on the discussion in the previous paragraph equation (4) can be satisfactorily used to determine the submergence.

i.e $\qquad S_t = 0.45V^2b^{-0.56} + 2.3C_f - B - R$ ....(4)

So on substituting $\quad V = 10.4$ m/s...........(from eq 13)

$\qquad\qquad\qquad b = 6$ (from turbine data)

$\qquad\qquad\qquad C_f = 0.57$ (Planned load factor)

$\qquad\qquad\qquad B = 9.7245$ m

$\qquad\qquad\qquad R = 2.2$ (SS overlay)

We get $\qquad S_t = (0.45*10.4^2* 6^{-0.56}) + (2.3*0.57) - 9.7245 - 2.2$

$\qquad\qquad\quad S_t = 7.2315$ m ....(18)

So the theoretical submergence as calculated from the equation (4) comes out to be $S_t = 7.2315$ but as Chilla Hydro Power Project is on the Ganga river which contains a lot of silt thus water in monsoon is highly rich in silt concentration thereby leading to enhancement in cavitation erosion . Therefore cavitation erosion is enhanced by the silt laden flow , so taking care for this it is

better to use the mean value between none to minimal cavitation and lower limit of cavitation of the IEC cavitation guarantee range to determine the submergence which can be than used to calculate the mass loss from the suction side of the turbine .

Thus the submergence value $= (6.3864 + 9.32028)/2$

$$= 7.85334 \text{ m} \dots\dots\dots\dots\dots(19)$$

Fig 5.7 Transverse section through the centerline of the unit of Chilla

5.4 DETERMINING CAVITATION EROSION FOR THE TURBINE ON SUCTION SIDE

As we have determined different submergence levels for the hydro turbine at the Chilla Hydro Power Project now it is necessary to determine the cavitation erosion for these determined turbine submergence levels using equation (10) discussed in Chapter 4

i.e $$W_t = k_2 d^2 \; 2.718^m \dots\dots\dots\dots\dots\dots\dots\dots(10)$$

$k_2 = 1$(median value) to be used for runner throat dia greater than 7 m

$= 5$, to be 75 per cent certain that the cavitation will be less than calculated

$= 10$, to be 95 per cent certain that cavitation will be less than calculated

and value of the cavitation exponent (m) can be calculated using (9)

i.e $$m = 0.45V^2 b^{-0.56} + 2.3C_f - B - R_l - S \dots\dots\dots\dots\dots\dots(9)$$

Using the respective values from their respective locations

i.e

$V = 10.4$ m/s...........(from eq 13)

$b = 6$ (from turbine data)

$C_f = 0.57$ (Planned load factor)

$B = 9.7245$ m

$R_l = 3.8$ (SS overlay)

1. For actual submergence , $S_a = 6.984$ m

$$m = (0.45*10.4^2*6^{-0.56}) + (2.3*0.57) - 9.7245 - 3.8 - 6.984$$

$$m = - 1.3525$$

And again substituting the value of cavitation index (m) in (10) we will get cavitation erosion as follows:

$$W = 1* 4^2 * 2.719^{-1.3525}$$

$$W = 4.136 \, Kg$$

Now using different values for k_2 as follows we get the weight of metal lost during period of 8000 hours

- For $k_2 = 1$ (median value)

We get the weight of metal lost during period of 8000 hours

W = 4.136 Kg

- For k_2 = 5 , to be 75per cent certain that the cavitation will be less than calculated

  Weight of metal lost during period of 8000 hours

  W = 4.136 x 5

  W = 20.68 Kg

- For k_2 = 10, to be 95 per cent certain that cavitation will be less than calculated

  Weight of metal lost during period of 8000 hours

  W = 4.136 x 10

  W = 41.36 Kg

2. Similarly for theoretical submergence S_t = 7.2314 m as in (18)

$$m = (0.45*10.4^2*6^{-0.56}) + (2.3*0.57) - 9.7245 - 3.8 - 7.2314$$

$$m = -1.5999$$

And again substituting the value of cavitation index (m) in (10) we will get cavitation erosion as follows:

$$W = 1* 4^2 * 2.719^{-1.5999}$$

$$W = 3.2293 \text{ Kg}$$

Now using different values for k_2 as follows we get the weight of metal lost during period of 8000 hours

- For k_2 = 1 (median value)

  We get the weight of metal lost during period of 8000 hours

  W = 3.2293 Kg

- For k_2 = 5 , to be 75per cent certain that the cavitation will be less than calculated

  Weight of metal lost during period of 8000 hours

68

W = 3.2293 x 5

W = 16.1465 Kg

- For $k_2 = 10$, to be 95 per cent certain that cavitation will be less than calculated

  Weight of metal lost during period of 8000 hours

  W = 3.2293 x 10

  W = 32.293 Kg

3. Similarly for submergence between mean value for none to minimal cavitation and lower limit of IEC cavitation guarantee range = 7.85334

$$m = (0.45*10.4^2*6^{-0.56}) + (2.3*0.57) - 9.7245 - 3.8 - 7.85334$$
$$m = -2.22192$$

And again substituting the value of cavitation index (m) in (10) we will get cavitation erosion as follows:

$$W = 1 * 4^2 * 2.719^{-2.22192}$$
$$W = 1.7334 \text{ Kg}$$

Now using different values for k_2 as follows we get the weight of metal lost during period of 8000 hours

- For $k_2 = 1$ (median value)

We get the weight of metal lost during period of 8000 hours

  W = 1.7334 Kg

- For $k_2 = 5$, to be 75per cent certain that the cavitation will be less than calculated

  Weight of metal lost during period of 8000 hours

  W = 1.7334 x 5

  W = 8.667 Kg

- For $k_2 = 10$, to be 95 per cent certain that cavitation will be less than calculated

  Weight of metal lost during period of 8000 hours

  W = 1.7334 x 10

W = 17.334 Kg

Now all the above analysis can shown in a tabulated form as follows

Table 5.3 Different submergence levels and corresponding mass loss with 75% and 95% confidence

Submergence in meters	Mass loss in Kgs	Mass loss in kgs and to be 75% certain that mass loss will be less than calculated	Mass loss in kgs and to be 95% certain that mass loss will be less than calculated
4.9895	30.4	152	304
6.3864	7.52	37.6	75.2
6.984	4.136	20.68	41.36
7.2314	3.2293	16.1465	32.293
7.85334	1.7334	8.667	17.334
9.32028	0.4	2	4

The mass loss calculated for the actual submergence i.e at 6.984 m is 41.36 kgs which is not an extravagant figure as during annual maintenance the mass of weld deposited on the turbine is near about 60 Kgs (as confirmed from the maintenance personals of Chilla). If turbine is set at a deeper level say 7.853 m than during annual maintenance a mass of about 24 kgs will be saved .

5.5 DETERMINING EFFICIENCY LOSS IN HYDRO TURBINE OF CHILLA DUE TO MASS LOSS CAUSED BY CAVITATION EROSION

The cavitation erosion which is most prominent for turbine erosion results in a decrease in turbine efficiency. Even one percent loss in turbine efficiency leads to remarkable decrease in power generation along with high economic losses. So considering efficiency as a consequence of mass loss the following model was observed [21].

$$Eff_{wl} = k \times M^{-a} \dots \dots \dots \dots \dots \dots (11)$$

Where ,

Eff_{wl} = predicted efficiency with mass loss

M = Mass loss

a = 0.00500250124054351

So it can be seen from the relation that mass loss is inversely proportional with a power raised to the efficiency . So to arrive at a trend to calculate the efficiency as a result of mass loss we can give that constant a value of 0.92 (the full load turbine efficiency).

To achieve at the optimistic side of the loss in efficiency due to mass loss we will be using 95% confidence values. Using equation (20) efficiency was calculated with corresponding mass losses and can be tabulated as follows

Table 5.4 Submergence and efficiency with corresponding mass loss for Chilla

Submergence in meters	Mass loss in kgs and to be 95% certain that mass loss will be less than calculated	M^{-a} where a = 0.00500250124054351	$Eff_{wl} = 0.92 \times M^{-a}$
4.9895	304	.9718	.89406
6.3864	75.2	.97862	.90
6.984	41.36	.98155	.903026
7.2314	32.293	.982	.90344
7.85334	17.334	.98583	.90696
9.32028	4	.99309	.91364

The relation between the submergence and the efficiency can be plotted and can be shown graphically as in the following figure 5.7
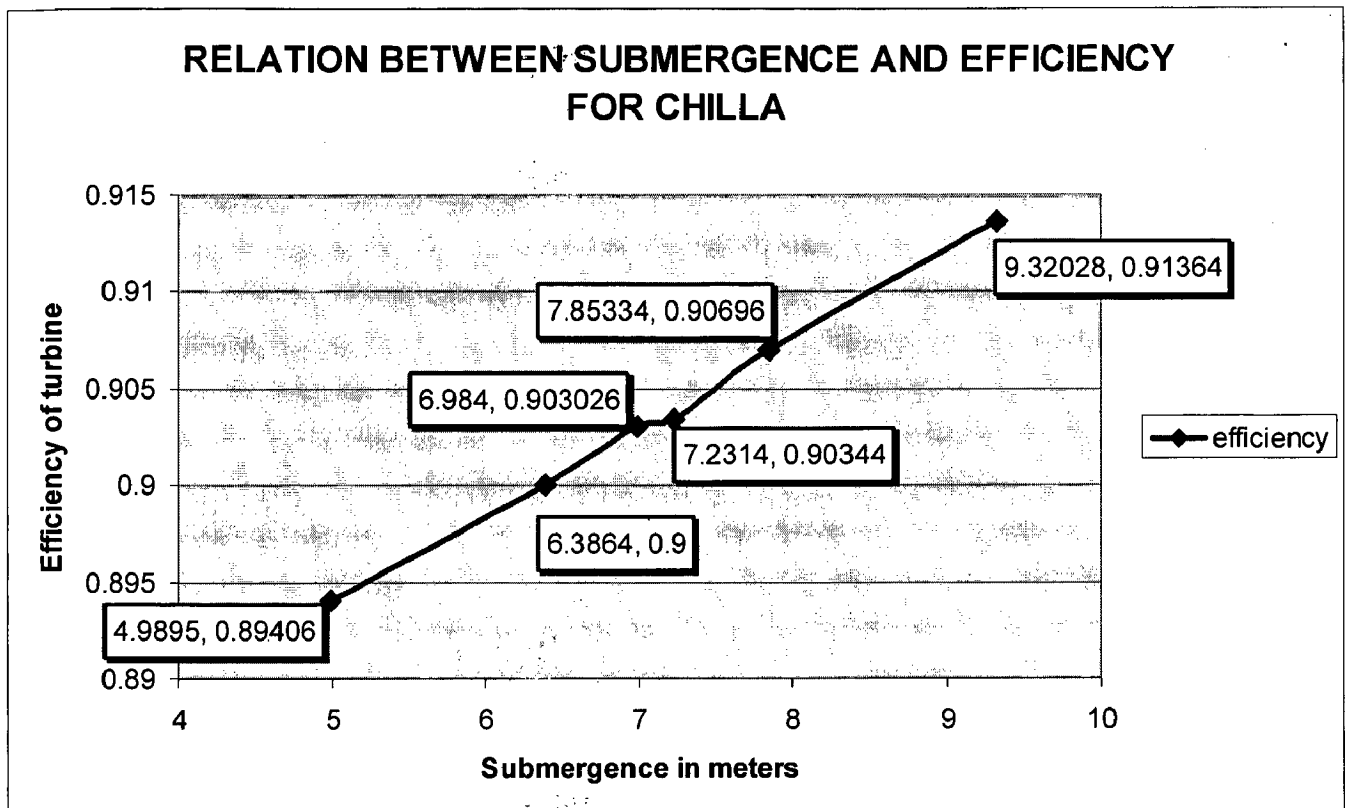

Fig 5.7 Relation between increasing submergence and efficiency for Chilla

5.6 ESTIMATING THE DECREASE IN POWER GENERATION DUE TO LOSS OF TURBINE EFFICIENCY

From the discussion and the table and fig it is evident that there will be a loss in efficiency when there is a mass loss in the turbine due to cavitation which in turn is again related the submergence or the turbine setting. Depending on the loss of efficiency there will be a loss in power generation which needs to be estimated . for estimating loss in power generation let's assume that annual generation (in 8760 hrs) is 725 MU (planned energy generation) at turbine full load efficiency that is 92%. So generation in 8000 hrs

= (725 x 8000)/8760

=662.1004566 MU

72

Considering that each turbine in the project contributes the same no. of units in power generation, and the loss in efficiency will be the same for all the four turbines so the efficiency calculated in table 5.4 can be directly multiplied by the units generated at efficiency of 92% so as to get the units generated at lesser efficiencies which can be tabulated as follows

Table 5.5 Submergence and corresponding units generated in 8000 hrs in Chilla

Submergence in meters	Eff$_{wl}$	No. of Units generated in 8000 hrs in Million units
4.9895	.89406	643.432
6.3864	.90	647.7069
6.984	.903026	649.8846
7.2314	.90344	650.1826
7.85334	.90696	652.71587
9.32028	.91364	657.523
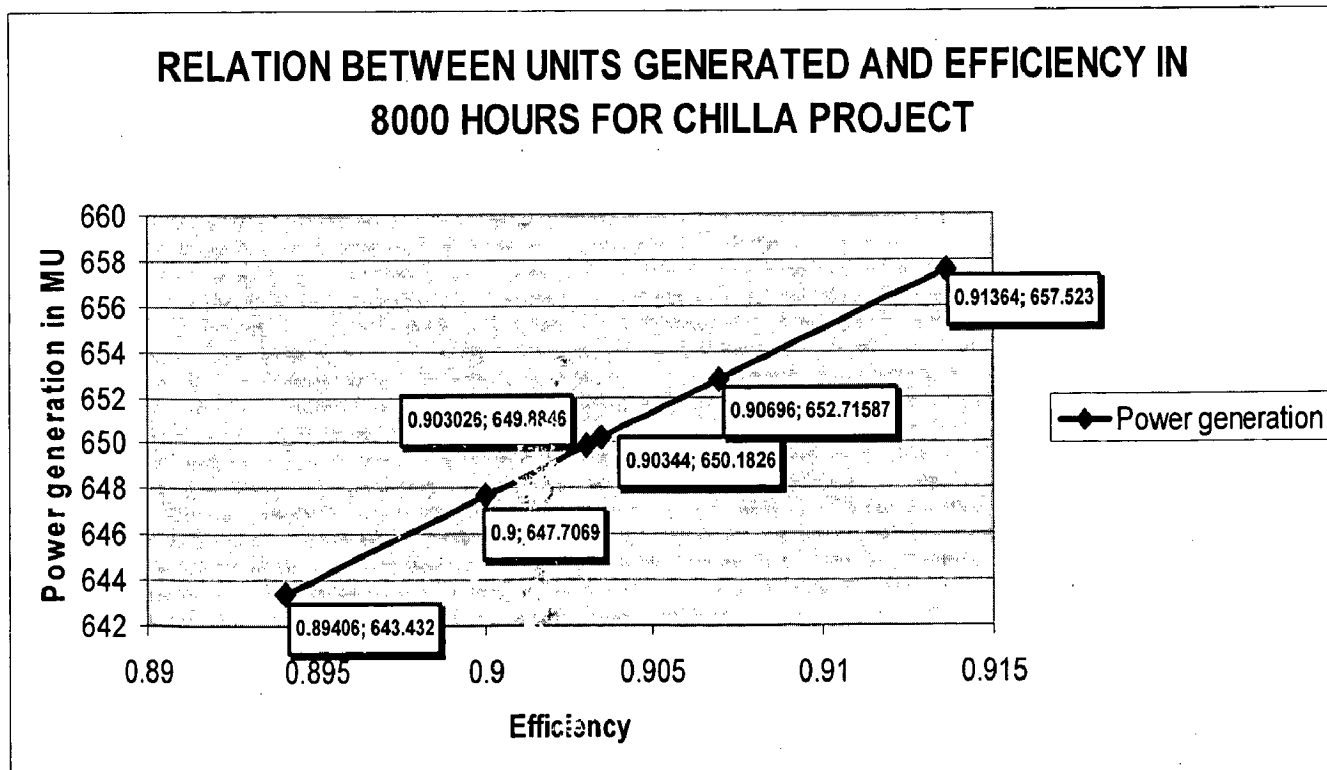
Fig 5.8 Relation between Units generated and efficiency in 8000 hrs for Chilla

73

Now the figures for the units generated at a lesser efiiciency due to cavitation erosion have been estimated but For giving a final picture it is required to calculate the loss in power generation per annum which can be calculated by subtracting the units generated at lesser efficiency from the units generated at full efficiency and can be tabulated as follows.

Table 5.6 Submergence and loss in power generation per annum in Chilla

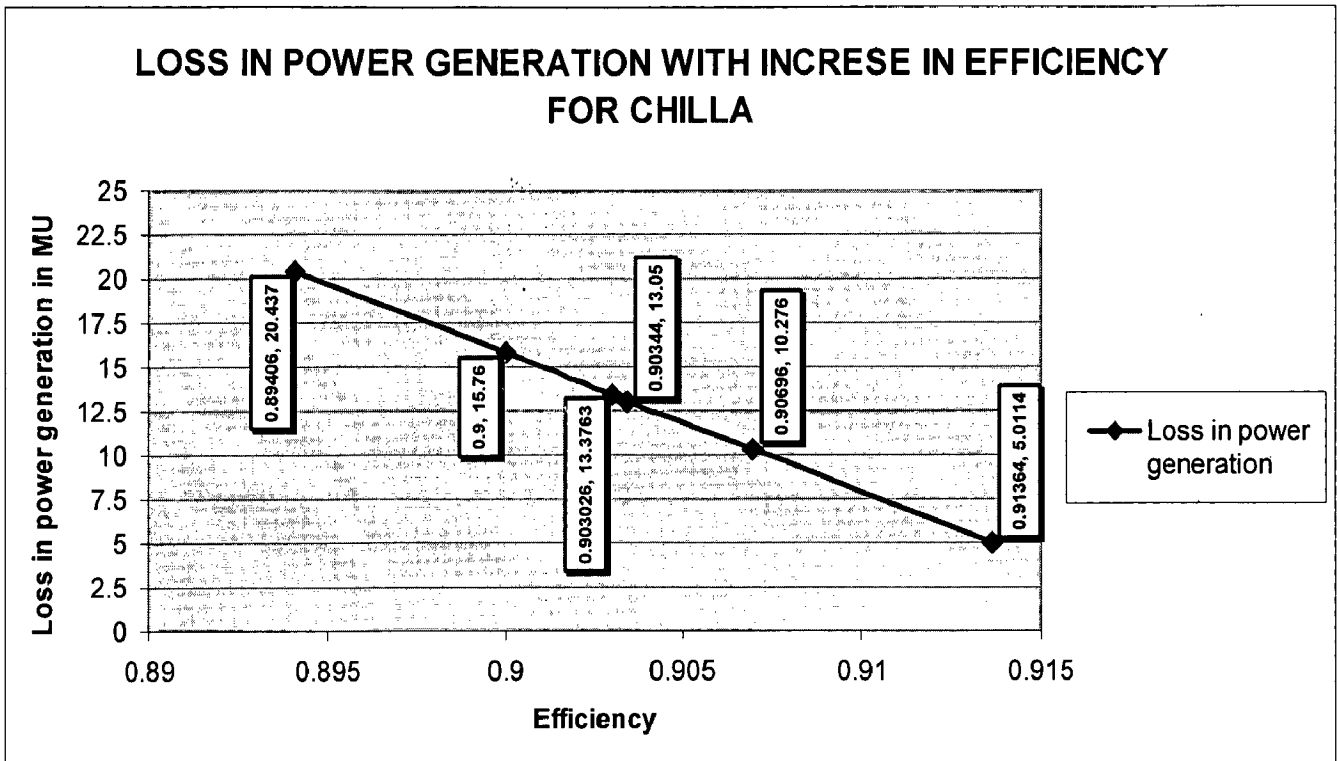| Submergence in meters	Eff_{wl}	Loss of Units generated in 8000 hrs in Million units	Loss of Units generated per annum in Million units
4.9895	.89406	18.6684	20.437
6.3864	.90	14.3935	15.76
6.984	.903026	12.2158	13.3763
7.2314	.90344	11.9178	13.05
7.85334	.90696	9.3846	10.276
9.32028	.91364	4.5766	5.0114

Fig 5.9 Relation between Loss in power generation per annum with efficiency of turbine for Chilla

Now the loss in power generation can be directly linked to the different submergence levels and can be plotted as shown in fig 5.10
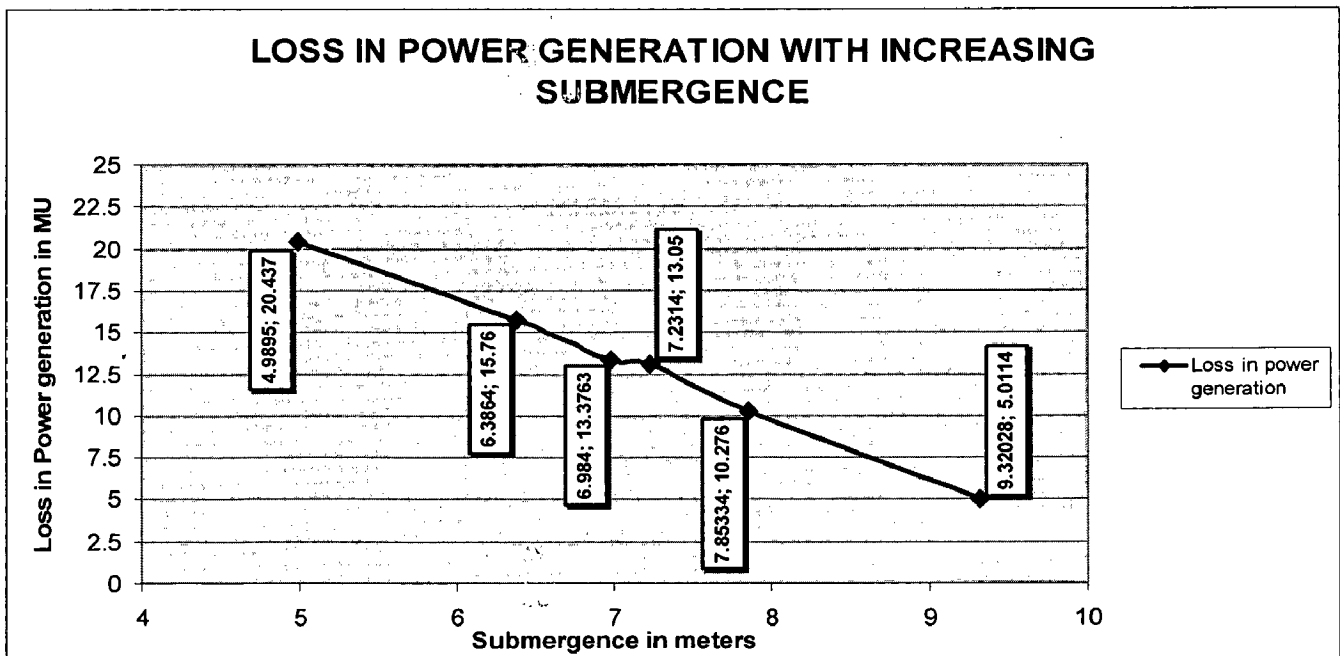

Fig 5.10 relation between loss in power generation with submergence for Chilla

And now the variation of efficiency and the power generation loss can be combined on the san graph with the increasing submergence as in fig 5.11
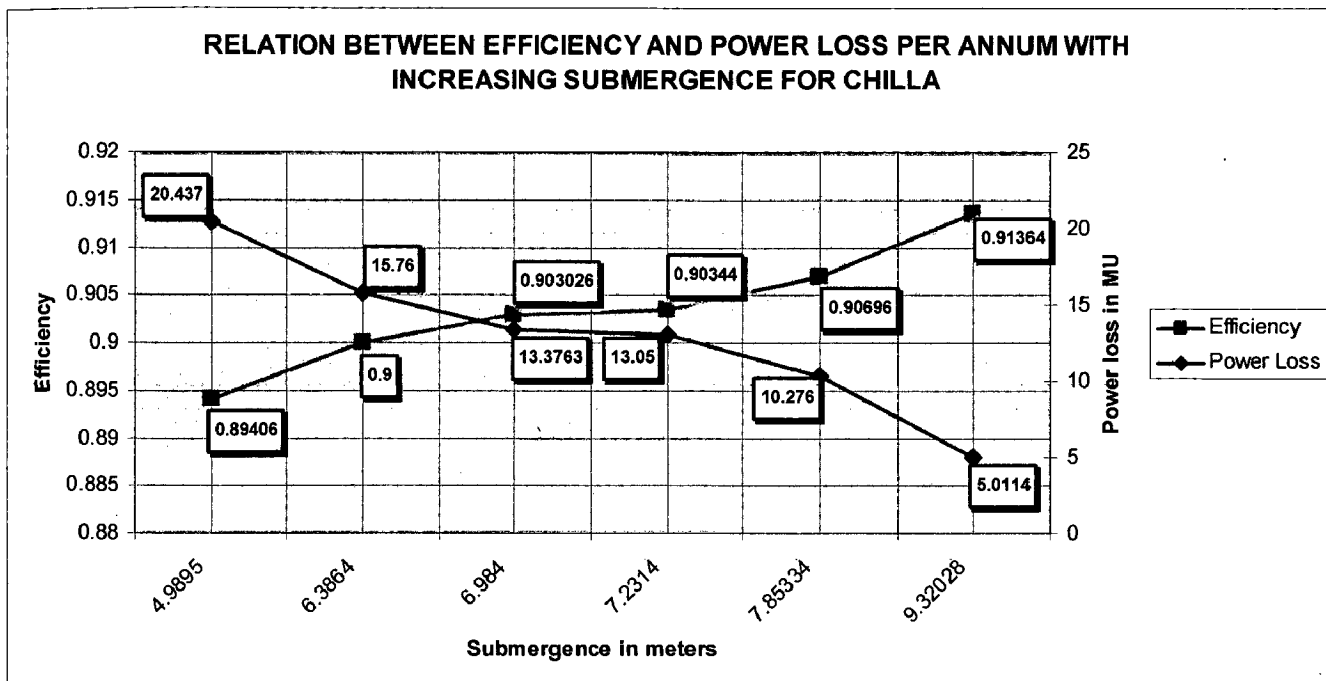
RELATION BETWEEN EFFICIENCY AND POWER LOSS PER ANNUM WITH INCREASING SUBMERGENCE FOR CHILLA

Fig 5.11 Relation between efficiency and power loss per annum with increasing submergence for Chilla

5.7 DETERMINING THEORITICAL SUBMERGENCE FOR DHUKWAN HYDR(PROJECT

5.7.1 Salient features of Dhukwan Hydro Project

The Dhukwan hydro power project is which is a project of U.P. Jal Vidyut Nigam Ltd. is located i the plains of Jhansi district of Uttar Pradesh which comprises of construction of a Power House (2 15 MW) at the toe of earthen bank of Dhukwan dam on river Betwa and is about 30 Km from Jhans:

Some of the required Salient Features Of the project as in the Detailed Project Repoi prerared by AHEC are as follows

| 1. | Name of Project | : | Dhukwan Hydro Power Project |

2. Location

	(a)	State	:	Uttar Pradesh
	(b)	District	:	Jhansi
	(c)	Village	:	Sukwan-Dhukwan

76

(d)	Access	:	Site is 30 km from Jhansi (All weather road)
	Nearest Rail Head (B.G.)	:	Jhansi, 30 Km from site

3. Geographical Coordinates

(a)	Longitude	:	$25^0 12'$ E
(b)	Latitude	:	$78^0 33'$ N
(c)	Reference toposheet	:	54 K/12/NW

4. Head	:	20.93m
Gross (weighted)	:	20.0 m
Net (weighted)	:	20.0 m
Design	:	20.0 m

5. Discharge	:	88 cumecs/turbine

6. Turbine

(a)	Type	:	Kaplan
(b)	Nos.	:	2
(c)	Capacity	:	16,500 Kw each
(d)	Speed	:	150 rpm
(e)	Runner Dia		3800 mm

7. Plant Usage Factor (As per availability of water)	:	44.38 %

8. Tail race water elevation	:	250 m (as from the layout of the project)

9. No. of runner blades	:	4 (assumed)

5.7.2 Calculations to determine turbine setting for the Dhukwan Project

Using equation Using equation (2) to determine B

ie. $\qquad B = 10.3 - 0.002E^{0.92} - 0.01T$

taking E = Tail water elevation = 250 m

and T = 20^0C

We get B = 9.78.................................(14)

Velocity at throat can be calculated using the power equation(12) which is as follows:

$$O = 9.81 \times 0.785d^2 \, Vhe$$

where O = the turbine full-load output at rated net head (kilowatts)

Substituting the values as

Runner Diameter (d) = 3.8 m

Net Rated head of the turbine (as per turbine specification) = 20.0 m

Taking Efficiency at full load (e) = 92 %

So substituting all required values in (12)

$$V = \frac{O}{9.81 * 0.785 * d^2 he}$$

$$V = 8.06418 \text{ m/s} \sim 8.0642 \text{ m/s} \dots\dots\dots\dots\dots(15)$$

Now substituting the Value of B and V from (14)and (15) respectively and

No. of runner blades(b) = 4   (assumed for turbine)

Value of R for stainless steel runners = 2.9

And the plant usage factor C_f = 0.4438 (from the DPR data)

In equation (4) to determine theoretical submergence

$$S_t = (0.45 * 8.0642^2 * 4^{-0.56}) + (2.3 * 0.4438) - 9.78 - 2.9$$

$$S_t = 1.80074 \sim 1.8 \text{ m} \dots\dots\dots\dots\dots\dots(16)$$

CHAPTER-6

CONCLUSIONS

In order to estimate the losses caused by the cavitation erosion and the impact of turbine setting or the submergence of the turbine a mathematical analysis based on the empirical relations was carried out for the Chilla Hydro Project. To carry out the analysis of the studied hydro power project data related to the setting of the turbine , annual energy generation and other required data were collected from the power house and based on the analysis carried out following results were drawn from the study .

(i)   The optimal submergence for the turbine based on the empirical relations , analysis and discussions comes out to be 7.853 m however the actual submergence of the turbine provided is 6.984 m

(ii)   Because of this difference in actual and determined turbine setting there will be an extra mass loss of approximately 24 kgs per 8000 hours of turbine operation.

(iii)   Due to this extra mass loss a percentage efficiency drop of about 0.44% is calculated in the turbine of Chilla .

(iv)   This drop in the efficiency of the turbine results in an annual loss of approximately 3.1 MU for the power house.

In conclusion it can be stated that if turbine is set at a greater depth of 7.853 m than 3.1003 MU per annum can be saved or in other words by changing the submergence of the turbine from 6.984 m to 7.853 m power generation can be increased by 3.1003 MU per annum. Thus a huge sum of revenue can be saved just by increasing the submergence of the turbine and moreover the weld material required during maintenance will be approximately 24 kgs less than what is required at present.

(v)   In addition of the case study of Chilla, optimum submergence for a new site Dhukwan was calculated using the empirical relations and an optimum submergence of 1.8 m is obtained .

The analysis was based only on the cavitation erosion whereas mass loss due to silt erosion should also be taken into account for achieving more realistic figures of power loss per annum . Moreover due to silt laden water cavitation is much more than expected and therefore combined action of silt and cavitation should also be taken care off and which can be a future part of this study.

REFERENCES

1. B.S. K Naidu *"Small hydro in India: environment friendly alternative energy source"* TERI Information Monitor on Environmental Science 1(2): 81–93.

2. Arne Kjølle, *"Mechanical Equipment"*, A survey,

3. Vidhu kumar Pande *"Effect of hydraulic design of Pelton turbines on damage due to silt erosion and its reduction"* , Executive Director , BHEL Bhopal

4. Mei Zu Yan , Tsinghua University China " *Protecting hydro turbines in silt laden river"*,Hydropower & Dams Issue Four,1996

5. B.S.K Naidu, Winrock International, India *"Addressing the problems of silt erosion at hydro plants"*,Hydropower & Dams,Issue three 1997.

6. B.S.K Naidu *"Silting problems in hydro power plants & their remedial solutions"*

7. D R Andrews , Cavendish Laboratory,University of Cambridge, *"Analysis of solid particle erosion mechanism"* ,Applied Physics. 14 (1981)

8. S. Singh, " *Operational problems and development of a new runner for silty water"*, Water Power & Dam Construction , November1990

9. Bhola Thapa & Hermod Brekke , *"Effect of sand particle size and surface curvature in erosion of hydro turbine"* , 22nd IAHR Symposium on Hydraulic Machinery and Systems June29-July 2, 2004 Stolkholm-Sweden

10. Xavier Escaler, Eduard Egusquiza, Mohamed Farhat, Franc-ois Avellan, Miguel Coussirat, *"Detection of cavitation in hydraulic turbines"*, Mechanical Systems and Signal Processing 20 (2006) 983–1007.

11. Timo KOIVULA, Tampere University of Technology, Institute of Hydraulics and Automation, Finland, *"On Cavitation in Fluid Power"*.

12. Mikael Grekula and Goran Bark,Chalmers University of Technology, Goteborg, Sweden, *"Experimental Study of Cavitation in a Kaplan Model Turbine"*

13. François AVELLAN, Professor ,Laboratory for Hydraulic Machines, School of Engineering.EPFL Swiss Federal Institute of Technology Lausanne, Switzerland, *"Intrduction to Cavitation in Hydraulic Machinery"*, The 6th International Conference on Hydraulic Machinery and Hydrodynamics Timisoara, Romania, October 21 - 22, 2004

14. N. Berchiche, J.P. Franc, J.M. Michel, *"A Cavitation Erosion Model for Ductile Materials"*, CAV2001:sessionA3.001

15. J Klastrup Kristensen, I Hansson and KA Mmch, Laboratory of Applied Physics I, Technical University of Denmark, Lyngby, Denmark, *"A simple model for cavitation erosion of metals"*, 30 Nov 1977

16. J.L Gordon, Consulting Engineer, *"Determining Turbine runner metal loss caused by cavitation erosion"* , Water Power & Dam Construction , August 1991.

17. H. Soyama, H. Kumano and M. SakH. Saka Tohoku University, Sendai 980-8579, Japan, *"A New Parameter to Predict Cavitation Erosion"*, CAV2001:sessionA3.002.

18. Lu Li (Institute of Water Conservancy and Hydroelectric Power Research), Huang Jitang Xu Xieqing,(Tsinghua University), *"Bubble Collapse in Solid-liquid Two-Phase Fluid"*

19. Shengcai LI,Fluid Dynamics Research Centre,Warwick University, UK, *"Cavitation Enhancement in Silt erosion; Obstacles & Way Forward"*, Fifth International Symposium on Cavitation (CAV2003) Osaka, Japan, November 1-4, 2003

20. J. L. Gordon, Member, ASCE, *"Hydroturbine Cavitation Erosion"*, Journal of Energy Engineering, Vol. 118, No. 3, December, 1992. ©ASCE

21. Tri Ratna Bajracharya,Chandra Bahadur Joshi, R.P.Saini and Ole Gunnar Dahlhaug, *"Correlation between Sand led erosion of Pelton Buckets and Efficiency losses in High Head Hydropower Schemes"*, Doctoral Research at the Instiute of Enginering, Kathmandu , Nepal.

22. Detailed Project Report of *"Dhukwan Hydro power project on river Betwa"*Prepared by AHEC, IIT Roorkee